Discrete Mechanics and Optimal Control for Constrained Systems (DMOCC)

Sigrid Leyendecker*
Aeronautics and Control and Dynamical Systems
California Institute of Technology 205-45
Pasadena, CA 91125
email: sleye@caltech.edu

Sina Ober-Blöbaum†
Control and Dynamical Systems
California Institute of Technology 107-81
Pasadena, CA 91125
email: sinaob@cds.caltech.edu

Jerrold E. Marsden‡
Control and Dynamical Systems
California Institute of Technology 107-81
Pasadena, CA 91125
email: jmarsden@caltech.edu

Michael Ortiz§
Aeronautics and Mechanical Engineering
California Institute of Technology 105-50
Pasadena, CA 91125
email: ortiz@aero.caltech.edu

This version: July 15, 2008

*Research partially supported by ...
†Research partially supported by AFOSR Contract FA9550-08-1-0173.
‡Research partially supported by AFOSR Contract FA9550-08-1-0173.
§Research partially supported by ....

Abstract

The equations of motion of a controlled mechanical system subject to holonomic constraints may be formulated in terms of the states and controls by applying a constrained version of the Lagrange-d'Alembert principle. This paper derives a structure preserving scheme for the optimal control of such systems using, as one of the key ingredients, a discrete analogue of that principle. This property is inherited when the system is reduced to its minimal dimension by the discrete null space method. Together with initial and final conditions on the configuration and conjugate momentum, the reduced discrete equations serve as nonlinear equality constraints for the minimisation of a given objective functional. The algorithm yields a sequence of discrete configurations together with a sequence of actuating forces, optimally guiding the system from the initial to the desired final state. In particular, for the optimal control of multibody systems, a force formulation consistent with the joint constraints is introduced. This enables one to prove the consistency of the evolution of momentum maps. The method is applied to a satellite reorientation manoeuvre and a biomotion problem.

Contents

1 Introduction

This work combines two recently developed methods, namely the discrete null space method which is suitable for the accurate, robust and efficient time integration of constrained dynamical systems (in particular for multibody dynamics) and an approach to discrete mechanics and optimal control (DMOC) based on a discretisation of the Lagrange-d'Alembert principle. The idea of this combination has been introduced briefly in Leyendecker et al. [2007] and is investigated in detail for three-dimensional multibody systems consisting of rigid bodies interconnected by joints in this work.

From various available methods used to enforce holonomic constraints in the framework of the Hamiltonian or Lagrangian formalism (see for example, Bertsekas [1995]; Luenberger [1984] and for a computational approach Leyendecker et al. [2004]), the focus in this paper is on two methods yielding exact constraint fulfilment, the Lagrange multiplier method and a null space method, described in, for example, Benzi et al. [2005].

Because of the relatively simple structure of the evolution equations derived from the Lagrange multiplier method, their temporal discrete form can be derived easily using mechanical integrators as demonstrated among others in Betsch and Steinmann [2002]; Gonzalez [1999]; Wendlandt and Marsden [1997]. However, the presence of Lagrange multipliers amongst the set of unknowns enlarges the number of equations and causes the discrete system to be ill-conditioned for small time-steps as reported (amongst others) by Petzold and Lostedt [1986]; Hairer et al. [1989]. In contrast to this undesirable situation, the use of a specific null space method, especially in conjunction with a reparametrisation in generalised coordinates, has the advantageous property of a small dimensional system of equations. On the other hand, these evolution equations have a highly complicated structure, causing the derivation of their temporal discrete form to be expensive and therefore, in most cases, not recommended Leimkuhler and Reich [2004]; Rheinboldt [1997].

A remedy for these difficulties is found in the discrete null space method introduced in Betsch [2005], which proposes a reversal of two of the main steps when designing a specific numerical method. In the first step, the discrete form of the simple structured DAEs resulting from the use of the Lagrange multiplier method is derived using a mechanical integrator, e.g. an energy-momentum conserving integrator Betsch and Steinmann [2002]; Gonzalez [1999] or a variational integrator leading to a symplectic-momentum conserving scheme Wendlandt and Marsden [1997]. For forced systems, both methods correctly compute the change in momentum maps. Then, in the second step, the transition to the reduced scheme and finally the nodal reparametrisation are performed in the temporal discrete setting in complete analogy to the procedure de-

scribed in the continuous case according to the discrete null space method. The resulting time-stepping scheme performs excellently in all relevant categories. First of all, it yields the smallest possible dimension for the system of equations, promising lower computational costs than other schemes. Secondly, it is second order accurate and inherits the conservation properties from the constrained scheme and thirdly, the condition number of the scheme is independent of the time-step. Summarising, the discrete null space method is especially suited for the accurate simulation of large dimensional systems subject to a large number of constraints. In particular the resulting equations lend themselves as dynamic constraints in an optimisation algorithm since their dimension is minimal, thus only the exactly required number of unknowns has to be determined.

```
Jerry:  What the two steps were that get reversed gets lost
in the exposition.  Needs clarification.  You might even say:
Step 1...  and Step 2...  to be very clear.
```

ToDo

To find local solutions of nonlinear optimal control problems consisting of a given objective functional and equations describing the underlying dynamics of the system, a numerical method falling into the class of direct methods is used here. Thereby, the state and control variables are discretised directly in order to transform the optimal control problem into

```
Jerry:  "Transform" needs clarification:  transform
into...should be "discretize"?
```

ToDo

a finite dimensional nonlinear constrained optimisation problem that can be solved by standard nonlinear optimisation techniques such as sequential quadratic programming (see Gill et al. [1997, 2000]; Schittkowski [1980]). In contrast to other methods like, e.g. shooting Stoer and Bulirsch [2002]; Kraft [1985]; Hicks and Ray [1971], multiple shooting Deuflhard [1974]; Bock and Plitt [1984]; Leineweber et al. [2003], or collocation methods von Stryk [1991]; Biegler [1984], relying on a direct integration of the associated ordinary differential equations or on its fulfilment at certain grid points (see also Betts [1998] and Binder et al. [2001] for an overview of the current state of the art), a recently developed method DMOC (Discrete Mechanics and Optimal Control—see Ober-Blöbaum [2008]; Junge et al. [2005]) is used here. It is based on the discretisation of the variational structure of the mechanical system directly. In the context of variational integrators, as in Marsden and West [2001], the discretisation of the Lagrange-d'Alembert principle leads to structure preserving time stepping equations which serve as equality constraints for the resulting finite dimensional nonlinear optimisation problem. In Junge et al. [2005]; Junge

and Ober-Blöbaum [2005, 2006] DMOC was first applied to low orbital thrust transfers and the optimal control of formation flying satellites including an algorithm that exploits a hierarchical structure of that problem. In Kanso and Marsden [2005], it has been applied to a multibody system representing an articulated swimmer and was formulated in generalised coordinates.

In this work, DMOC is used to find optimal trajectories of state and control variables for systems of rigid bodies subject to joint constraints. Each rigid body is viewed as a constrained continuum, i.e. it is described in terms of redundant coordinates subject to holonomic constraints Betsch and Steinmann [2001]; Reich [1996]. Then the equations of motion assume the form of DAEs with a constant mass matrix. Their temporal discrete form can be derived and reduced according to the discrete null space method. This procedure has the advantage of circumventing the difficulties associated with rotational parameters Betsch et al. [1998]; Bauchau and Trainelli [2003] and it can be generalised easily to the modelling of geometrically exact beams and shells and to multibody systems consisting of theses structures as developed in Leyendecker et al. [2006]; Betsch and Leyendecker [2006]; Leyendecker et al. [2008a]. The reduced time-stepping equations then serve as constraints in the optimisation algorithm.

The combination of the two proposed methods involves several specific benefits. First of all, the discrete dynamics constraints required to solve the optimal control problem using DMOC can be formulated easily. Using the discrete Lagrange-d'Alembert principle, they are derived as the discrete analogue to the simple structured evolution equations where the configuration constraints are enforced using Lagrange multipliers. Secondly, the discrete null space method reduces the dynamics constraints to the smallest possible number of equations and variables which leads to lower computational costs for the optimisation algorithm. Thirdly, the benefit of exact constraint fulfilment and correct computation of the change in momentum maps is guaranteed by the optimisation algorithm. These benefits are important, especially for high dimensional rigid body systems with joint constraints.

An outline of the paper is as follows. §2 fixes the formulation of the continuous optimal control problem of constrained dynamics which is formulated in the discrete setting in §3. Techniques for rigid body systems are set up in §4. The constrained formulation of the dynamics of kinematic pairs and the associated reduction of the equations of motion via the discrete null space method with nodal reparametrisation is reviewed in §5. The main contribution is contained in §6, which applies the theory developed in the paper to the optimal control of multibody systems. In particular, actuating forces being consistent with the specific joint constraints are given and structure preservation of the resulting time-stepping scheme is proved. Numerical examples from the field of satellite

reorientation maneuvers and biomotion are presented in §7.

2 Constrained Dynamics & Optimal Control

This section derives the equations of motion for forced holonomically constrained systems; these equations are to be fulfilled as constraints in the optimisation problem. The transformation of the differential algebraic equations by the null space method with reparametrisation, and in particular the equivalence of the resulting equations of motion, is described in detail in Leyendecker et al. [2008b] for conservative systems.

Consider an n-dimensional mechanical system with the time-dependent configuration vector $\boldsymbol{q}(t) \in Q$ and velocity vector $\dot{\boldsymbol{q}}(t) \in T_{q(t)}Q$, where $t \in [t_0, t_N] \subset \mathbb{R}$ denotes the time and $N \in \mathbb{N}$. Let the configuration be constrained by the function $\boldsymbol{g}(\boldsymbol{q}) = \boldsymbol{0} \in \mathbb{R}^m$ with constraint manifold

$$C = \{\boldsymbol{q} \in Q \mid \boldsymbol{g}(\boldsymbol{q}) = \boldsymbol{0}\} \tag{2.1}$$

and influenced by the force field $\boldsymbol{f} : \mathbb{R}^{n-m} \times TQ \to T^*Q$.

The Optimisation Problem. The goal is to determine the optimal trajectory and force field, such that the system is moved from the initial state $(\boldsymbol{q}^0, \dot{\boldsymbol{q}}^0) \in TC$ to the final state $(\boldsymbol{q}^N, \dot{\boldsymbol{q}}^N) \in TC$, obeying the equations of motion and at the same time, the objective functional

$$J(\boldsymbol{q}, \dot{\boldsymbol{q}}, \boldsymbol{f}) = \int_{t_0}^{t_N} B(\boldsymbol{q}, \dot{\boldsymbol{q}}, \boldsymbol{f})\, dt \tag{2.2}$$

is to be minimised. Here, $B(\boldsymbol{q}, \dot{\boldsymbol{q}}, \boldsymbol{f}) : TC \times T^*Q \to \mathbb{R}$ is a given cost function.

```
Jerry:  Make sure the domain of B is correct.
```

ToDo

The Constrained Lagrange-d'Alembert Principle. As we have mentioned, the motion has to obey the equations of motion which, in the present case, are based on a constrained version of the Lagrange-d'Alembert principle (see e.g. Marsden and Ratiu [1999]), which requires that

$$\delta \int_{t_0}^{t_N} L(\boldsymbol{q}, \dot{\boldsymbol{q}}) - \boldsymbol{g}^T(\boldsymbol{q}) \cdot \boldsymbol{\lambda}\, dt + \int_{t_0}^{t_N} \boldsymbol{f} \cdot \delta\boldsymbol{q}\, dt = 0 \tag{2.3}$$

for all variations $\delta\boldsymbol{q} \in TQ$ vanishing at the endpoints and $\delta\boldsymbol{\lambda} \in \mathbb{R}^m$. The Lagrangian $L : TQ \to \mathbb{R}$ equals the kinetic energy $\frac{1}{2}\dot{\boldsymbol{q}}^T \cdot \boldsymbol{M} \cdot \dot{\boldsymbol{q}}$ including the

consistent mass matrix $\boldsymbol{M} \in \mathbb{R}^{n\times n}$ minus a potential function $V : Q \to \mathbb{R}$. Furthermore, $\boldsymbol{\lambda}(t) \in \mathbb{R}^m$ represents the vector of time dependent Lagrange multipliers. The last term represents the virtual work of the resulting from the force field. The constrained Lagrange-d'Alembert principle (2.3) leads to the differential-algebraic system of equations of motion

$$\begin{aligned} \frac{\partial L(\boldsymbol{q},\dot{\boldsymbol{q}})}{\partial \boldsymbol{q}} - \frac{d}{dt}\left(\frac{\partial L(\boldsymbol{q},\dot{\boldsymbol{q}})}{\partial \dot{\boldsymbol{q}}}\right) - \boldsymbol{G}^T(\boldsymbol{q})\cdot\boldsymbol{\lambda} + \boldsymbol{f} &= \boldsymbol{0} \\ \boldsymbol{g}(\boldsymbol{q}) &= \boldsymbol{0}, \end{aligned} \tag{2.4}$$

where $\boldsymbol{G}(\boldsymbol{q}) = D\boldsymbol{g}(\boldsymbol{q})$ denotes the Jacobian of the constraints. The vector $-\boldsymbol{G}^T(\boldsymbol{q})\cdot\boldsymbol{\lambda}$ represents the constraint forces that prevent the system from deviations of the constraint manifold.

The Null Space Method. Assuming that the constraints are independent, for every $\boldsymbol{q} \in C$ the basis vectors of $T_{\boldsymbol{q}}C$ form an $n \times (n-m)$ matrix $\boldsymbol{P}(\boldsymbol{q})$ with corresponding linear map $\boldsymbol{P}(\boldsymbol{q}) : \mathbb{R}^{n-m} \to T_{\boldsymbol{q}}C$. This matrix is called null space matrix, since

$$\operatorname{range}\left(\boldsymbol{P}(\boldsymbol{q})\right) = \operatorname{null}\left(\boldsymbol{G}(\boldsymbol{q})\right) = T_{\boldsymbol{q}}C. \tag{2.5}$$

Thus, a premultiplication of the differential equation $(2.4)_1$ by $\boldsymbol{P}^T(\boldsymbol{q})$ eliminates the constraint forces including the Lagrange multipliers from the system. The resulting equations of motion read

$$\begin{aligned} \boldsymbol{P}^T(\boldsymbol{q})\cdot\left[\frac{\partial L(\boldsymbol{q},\dot{\boldsymbol{q}})}{\partial \boldsymbol{q}} - \frac{d}{dt}\left(\frac{\partial L(\boldsymbol{q},\dot{\boldsymbol{q}})}{\partial \dot{\boldsymbol{q}}}\right) + \boldsymbol{f}\right] &= \boldsymbol{0} \\ \boldsymbol{g}(\boldsymbol{q}) &= \boldsymbol{0}. \end{aligned} \tag{2.6}$$

Reparametrisation. For many applications, it is possible to find a local parametrisation of the constraint manifold $\boldsymbol{F} : U \subseteq \mathbb{R}^{n-m} \to C$ in terms of independent generalised coordinates $\boldsymbol{u} \in U$. Then the Jacobian $D\boldsymbol{F}(\boldsymbol{u})$ of the coordinate transformation plays the role of a null space matrix. Since the constraints $(2.6)_2$ are fulfilled automatically by the reparametrised configuration variable $\boldsymbol{q} = \boldsymbol{F}(\boldsymbol{u})$, the system is reduced to $n-m$ second order differential equations. Due to the presence of constraints, the forces $\boldsymbol{f}$ are not independent. They can be calculated in terms of the time dependent generalised control forces $\boldsymbol{\tau}(t) \in T^*U$. Consequently, there are $n-m$ independent generalised forces acting on the generalised degrees of freedom. These can be calculated as $\boldsymbol{\tau} = \left(\frac{\partial \boldsymbol{F}}{\partial \boldsymbol{u}}\right)^T \cdot \boldsymbol{f}$, see e.g. Goldstein et al. [2002]. On the other hand, a redundant force vector $\boldsymbol{f} \in T^*Q$ can be computed via

$$\boldsymbol{f} = \boldsymbol{B}^T(\boldsymbol{q})\cdot\boldsymbol{\tau}, \tag{2.7}$$

with the $n \times (n-m)$ configuration dependent input transformation matrix $\boldsymbol{B}^T : T^*U \to T^*Q$. Thereby, the choice of the transformation matrix must ensure consistency of momentum maps in the sense that they change only and exactly according to the generalised force.

```
Jerry:  Equation (2.7) perhaps to be modified according to
our discussions
```

ToDo

3 Constrained discrete dynamics and optimal control

Analogous steps are performed in the temporal discrete variational setting to derive the forced constrained discrete Euler-Lagrange equations and their reduction to minimal dimension. Again, these steps have been investigated in detail in Leyendecker et al. [2008b] for conservative systems.

Corresponding to the configuration manifold Q, the discrete phase space is defined by $Q \times Q$ which is locally isomorphic to TQ. For a constant time-step $h \in \mathbb{R}$, a path $\boldsymbol{q} : [t_0, t_N] \to Q$ is replaced by a discrete path $\boldsymbol{q}_d : \{t_0, t_0+h, , \ldots, t_0+Nh = t_N\} \to Q$, $N \in \mathbb{N}$, where $\boldsymbol{q}_n = \boldsymbol{q}_d(t_n)$ is viewed as an approximation to $\boldsymbol{q}(t_n)$ at $t_n = t_0 + nh$. Similarly, $\boldsymbol{\lambda}_n = \boldsymbol{\lambda}_d(t_n)$ approximates the Lagrange multiplier, while the force field $\boldsymbol{f}$ is approximated by two discrete forces $\boldsymbol{f}_n^-, \boldsymbol{f}_n^+ : T^*U \times Q \to T^*Q$ in a way that respects work, as is explained below.

Discrete Constrained Lagrange-d'Alembert Principle. According to the derivation of variational integrators for constrained dynamics in Leyendecker et al. [2008b], the action integral in (2.3) is approximated in a time interval $[t_n, t_{n+1}]$ using the discrete Lagrangian $L_d : Q \times Q \to \mathbb{R}$ and the discrete constraint function $\boldsymbol{g}_d : Q \to \mathbb{R}$ via

$$L_d(\boldsymbol{q}_n, \boldsymbol{q}_{n+1}) - \frac{1}{2}\boldsymbol{g}_d^T(\boldsymbol{q}_n) \cdot \boldsymbol{\lambda}_n - \frac{1}{2}\boldsymbol{g}_d^T(\boldsymbol{q}_{n+1}) \cdot \boldsymbol{\lambda}_{n+1} \approx \int_{t_n}^{t_{n+1}} L(\boldsymbol{q}, \dot{\boldsymbol{q}}) - \boldsymbol{g}^T(\boldsymbol{q}) \cdot \boldsymbol{\lambda}\, dt. \tag{3.1}$$

Among various possible choices to approximate this integral, in this work the midpoint rule is used for the Lagrangian, i.e.

$$L_d(\boldsymbol{q}_n, \boldsymbol{q}_{n+1}) = hL\left(\frac{\boldsymbol{q}_{n+1} + \boldsymbol{q}_n}{2}, \frac{\boldsymbol{q}_{n+1} - \boldsymbol{q}_n}{h}\right) \tag{3.2}$$

and for the constraints

$$\boldsymbol{g}_d^T(\boldsymbol{q}_n) = h\boldsymbol{g}^T(\boldsymbol{q}_n) \tag{3.3}$$

is used. Likewise, the virtual work is approximated by

$$\boldsymbol{f}_n^- \cdot \delta\boldsymbol{q}_n + \boldsymbol{f}_n^+ \cdot \delta\boldsymbol{q}_{n+1} \approx \int_{t_n}^{t_{n+1}} \boldsymbol{f} \cdot \delta\boldsymbol{q}\, dt, \tag{3.4}$$

where $\boldsymbol{f}_n^+, \boldsymbol{f}_n^-$ are called the left and right discrete forces, respectively. They are specified in (3.11).

The discrete version of the constrained Lagrange-d'Alembert principle (2.3) requires the discrete path $\{\boldsymbol{q}_n\}_{n=0}^N$ and multipliers $\{\boldsymbol{\lambda}_n\}_{n=0}^N$ to fulfill

$$\delta \sum_{n=0}^{N-1} L_d(\boldsymbol{q}_n, \boldsymbol{q}_{n+1}) - \frac{1}{2}\boldsymbol{g}_d^T(\boldsymbol{q}_n)\cdot\boldsymbol{\lambda}_n - \frac{1}{2}\boldsymbol{g}_d^T(\boldsymbol{q}_{n+1})\cdot\boldsymbol{\lambda}_{n+1} + \sum_{n=0}^{N-1} \boldsymbol{f}_n^- \cdot \delta\boldsymbol{q}_n + \boldsymbol{f}_n^+ \cdot \delta\boldsymbol{q}_{n+1} = 0 \tag{3.5}$$

for all variations $\{\delta\boldsymbol{q}_n\}_{n=0}^N$ and $\{\delta\boldsymbol{\lambda}_n\}_{n=0}^N$ with $\delta\boldsymbol{q}_0 = \delta\boldsymbol{q}_N = \boldsymbol{0}$, which is equivalent to the constrained forced discrete Euler-Lagrange equations

$$\begin{aligned} D_2 L_d(\boldsymbol{q}_{n-1}, \boldsymbol{q}_n) + D_1 L_d(\boldsymbol{q}_n, \boldsymbol{q}_{n+1}) - \boldsymbol{G}_d^T(\boldsymbol{q}_n) \cdot \boldsymbol{\lambda}_n + \boldsymbol{f}_{n-1}^+ + \boldsymbol{f}_n^- &= \boldsymbol{0} \\ \boldsymbol{g}(\boldsymbol{q}_{n+1}) &= \boldsymbol{0} \end{aligned} \tag{3.6}$$

for $n = 1, \ldots, N-1$ where $\boldsymbol{G}_d(\boldsymbol{q}_n)$ denotes the Jacobian of $\boldsymbol{g}_d(\boldsymbol{q}_n)$. Note that the time-stepping scheme (3.6) has not been deduced by discretising (2.4), but rather via a discrete variational principle.

The Discrete Null Space Method. The dimensional reduction of the time-stepping scheme (3.6) can be accomplished analogous to the continuous case according to the discrete null space method. To eliminate the discrete constraint forces from the equations, a discrete null space matrix fulfilling

$$\text{range}\,(\boldsymbol{P}(\boldsymbol{q}_n)) = \text{null}\,(\boldsymbol{G}_d(\boldsymbol{q}_n)) \tag{3.7}$$

is employed. As with equation (2.6), pre-multiplying (3.6) by the transposed discrete null space matrix cancels the constraint forces; i.e., the Lagrange multipliers are eliminated from the set of unknowns and the system's dimension is reduced to n. One gets

$$\begin{aligned} \boldsymbol{P}^T(\boldsymbol{q}_n) \cdot \left[D_2 L_d(\boldsymbol{q}_{n-1}, \boldsymbol{q}_n) + D_1 L_d(\boldsymbol{q}_n, \boldsymbol{q}_{n+1}) + \boldsymbol{f}_{n-1}^+ + \boldsymbol{f}_n^- \right] &= \boldsymbol{0} \\ \boldsymbol{g}(\boldsymbol{q}_{n+1}) &= \boldsymbol{0}. \end{aligned} \tag{3.8}$$

Nodal Reparametrisation. As in the continuous case, a reduction of the system to the minimal possible dimension can be accomplished by a local reparametrisation of the constraint manifold in the neighbourhood of the discrete configuration variable. At the time nodes, $\boldsymbol{q}_n$ is expressed in terms of

the discrete generalised coordinates $\boldsymbol{u}_n \in U \subseteq \mathbb{R}^{n-m}$ by the map $\boldsymbol{F} : U \subseteq \mathbb{R}^{n-m} \times Q \to C$, such that the constraints are fulfilled.

$$\boldsymbol{q}_n = \boldsymbol{F}(\boldsymbol{u}_n, \boldsymbol{q}_{n-1}) \quad \text{with} \quad \boldsymbol{g}(\boldsymbol{q}_n) = \boldsymbol{g}(\boldsymbol{F}(\boldsymbol{u}_n, \boldsymbol{q}_{n-1})) = \boldsymbol{0} \tag{3.9}$$

The discrete generalised control forces are assumed to be constant in each time interval, see Figure 3.1. First of all, the effect of the generalised forces acting in $[t_{n-1}, t_n]$ and in $[t_n, t_{n+1}]$ is transformed to the time node t_n via

$$\boldsymbol{\tau}_{n-1}^{+} = \frac{h}{2}\,\boldsymbol{\tau}_{n-1} \qquad \boldsymbol{\tau}_n^{-} = \frac{h}{2}\,\boldsymbol{\tau}_n. \tag{3.10}$$

Secondly, the components of the discrete force vectors $\boldsymbol{f}_{n-1}^{+}, \boldsymbol{f}_n^{-} \in T_{\boldsymbol{q}_n}^{*} C$ can be calculated similar to (2.7) as

$$\begin{aligned} \boldsymbol{f}_{n-1}^{+} &= \boldsymbol{B}^T(\boldsymbol{q}_n) \cdot \boldsymbol{\tau}_{n-1}^{+} \qquad \boldsymbol{f}_n^{-} = \boldsymbol{B}^T(\boldsymbol{q}_n) \cdot \boldsymbol{\tau}_n^{-} \\ \boldsymbol{f}_n &= \boldsymbol{f}_n^{+} + \boldsymbol{f}_n^{-} \\ \boldsymbol{f}_d &= \{\boldsymbol{f}_n\}_{n=0}^{N-1}. \end{aligned} \tag{3.11}$$

Thus $\boldsymbol{f}_{n-1}^{+}$ denotes the effect of the generalised force $\boldsymbol{\tau}_{n-1}$ acting in $[t_{n-1}, t_n]$ on $\boldsymbol{q}_n$ while $\boldsymbol{f}_n^{-}$ denotes the effect on $\boldsymbol{q}_n$ of $\boldsymbol{\tau}_n$ acting in $[t_n, t_{n+1}]$.

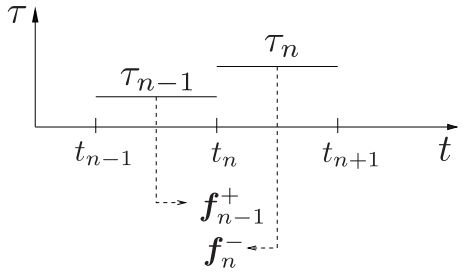

Figure 3.1: Relation of redundant forces $\boldsymbol{f}_{n-1}^{+}, \boldsymbol{f}_n^{-}$ at t_n to piecewise constant discrete generalised forces $\boldsymbol{\tau}_{n-1}, \boldsymbol{\tau}_n$.

Insertion of the nodal reparametrisation for the configuration (3.9) into the scheme redundantises $(3.8)_2$. The resulting scheme

$$\boldsymbol{P}^T(\boldsymbol{q}_n) \cdot \left[D_2 L_d(\boldsymbol{q}_{n-1}, \boldsymbol{q}_n) + D_1 L_d(\boldsymbol{q}_n, \boldsymbol{F}(\boldsymbol{u}_{n+1}, \boldsymbol{q}_n)) + \boldsymbol{f}_{n-1}^{+} + \boldsymbol{f}_n^{-} \right] = \boldsymbol{0} \tag{3.12}$$

has to be solved for $\boldsymbol{u}_{n+1}$ whereupon $\boldsymbol{q}_{n+1}$ is obtained from (3.9). (3.12) is equivalent to the constrained scheme (3.6), thus it also has the key properties of exact constraint fulfilment, symplecticity and momentum consistency, i.e. any change in the value of a momentum map reflects exactly the applied forces as will be shown in §7. When no load is present, momentum maps are

conserved exactly. While the constrained scheme (3.6) becomes increasingly ill-conditioned for decreasing time-steps, the condition number of (3.12) is independent of the time-step.

```
Jerry:  Perhaps give the equation number for "the constrained
scheme"
```

ToDo

Remark 3.1 (Stochastic Forces)**.** Variational integrators for stochastic mechanical systems driven by Wiener processes have been introduced in Bou-Rabee and Owhadi [2008]. There, the discrete Lagrangian is augmented by an approximation to the Stratonovic stochastic integral that represents the stochastic influence of the Wiener processes. In Bou-Rabee and Owhadi [2007], the idea has been generalised to constrained systems using variational partitioned symplectic Runge-Kutta integration and enforcing constraints using Lagrange multipliers. It is also possible to include the approximation to the Stratonovic stochastic integral in (3.1), yielding constrained stochastic discrete Euler-Lagrange equations of the form (3.6), in which the left and right discrete forces are determined according to a normal distribution $\mathcal{N}(0, h)$ of random variables in one time interval. The presence of stochastic forces does not influence the reduction procedure of the time-stepping scheme using the discrete null space method with nodal reparametrisation. Using the same randomly created forces, (3.6) and (3.12) are still equivalent. This has been verified numerically by simulating the stochastic dynamics of a pendulum. However, the corresponding results will be presented elsewhere and this work is restricted to the deterministic setting.

```
Jerry:  Perhaps some rewording is needed as it is not clear
that the exposition that follows uses the stochastic setting
or not.  Maybe with "Stochastic Forces" use a Remark or a
footnote.
```

ToDo

Boundary Conditions. In the next step, the boundary conditions $\boldsymbol{q}(t_0) = \boldsymbol{q}^0, \dot{\boldsymbol{q}}(t_0) = \dot{\boldsymbol{q}}^0$ and $\boldsymbol{q}(t_N) = \boldsymbol{q}^N, \dot{\boldsymbol{q}}(t_N) = \dot{\boldsymbol{q}}^N$ have to be formulated in the discrete setting. Let $\boldsymbol{q}_{00} \in C$ be a fixed reference configuration, relative to which the initial configuration is computed as $\boldsymbol{q}_0 = \boldsymbol{F}(\boldsymbol{u}_0, \boldsymbol{q}_{00})$. To prescribe an initial configuration at t_0, one can request $\boldsymbol{u}_0 = \boldsymbol{u}^0$. If an absolute reparametrisation is used, i.e. (3.9) is changed to $\boldsymbol{q}_n = \boldsymbol{F}(\boldsymbol{u}_n, \boldsymbol{q}_{00})$, then $\boldsymbol{u}_N = \boldsymbol{u}^N$ defines the final configuration $\boldsymbol{q}_N$ uniquely (see Sections 7.2 and 7.3 for examples). However, for the relative reparametrisation (3.9), $n - m$ independent final configuration conditions have to be identified with the function $\boldsymbol{D} : Q \times Q \to \mathbb{R}^{n-m}$ depending on the specific system under consideration (see §7.1 for an example).

Since in the present formulation of constrained forced discrete variational dynamics on $Q \times Q$, velocities are not properly defined, the velocity conditions have to be transformed into conditions on the conjugate momenta, which are defined at each and every time node using the discrete Legendre transform. Three different versions have been defined in Leyendecker et al. [2008b] for the conservative case. Now, the presence of forces at the time nodes has to be incorporated into that transformation leading to the constrained forced discrete Legendre transforms $\mathbb{F}^{cf^-}L_d : Q \times Q \to T^*Q$ and $\mathbb{F}^{cf^+}L_d : Q \times Q \to T^*Q$ reading

$$\begin{aligned}
&\mathbb{F}^{cf^-}L_d : (\boldsymbol{q}_n, \boldsymbol{q}_{n+1}) \mapsto (\boldsymbol{q}_n, \boldsymbol{p}_n^-) \\
&\qquad \boldsymbol{p}_n^- = -D_1 L_d(\boldsymbol{q}_n, \boldsymbol{q}_{n+1}) + \frac{1}{2}\boldsymbol{G}_d^T(\boldsymbol{q}_n) \cdot \boldsymbol{\lambda}_n - \boldsymbol{f}_n^- \\
&\mathbb{F}^{cf^+}L_d : (\boldsymbol{q}_{n-1}, \boldsymbol{q}_n) \mapsto (\boldsymbol{q}_n, \boldsymbol{p}_n^+) \\
&\qquad \boldsymbol{p}_n^+ = D_2 L_d(\boldsymbol{q}_{n-1}, \boldsymbol{q}_n) - \frac{1}{2}\boldsymbol{G}_d^T(\boldsymbol{q}_n) \cdot \boldsymbol{\lambda}_n + \boldsymbol{f}_{n-1}^+.
\end{aligned} \tag{3.13}$$

As in the conservative case, the time-stepping scheme $(3.6)_1$ can be interpreted as matching of momenta $\boldsymbol{p}_n^+ - \boldsymbol{p}_n^- = \boldsymbol{0}$ such that along the discrete trajectory, there is a unique momentum at each time node n which can be denoted by $\boldsymbol{p}_n$. However, just as the appearance of Lagrange multipliers is avoided in the discrete equations of motion (3.12), their presence in the initial and final momentum conditions complicates matters unnecessarily. Even though they can be related to the discrete trajectory via

$$\boldsymbol{\lambda}_n = \boldsymbol{R}_d^T(\boldsymbol{q}_n) \cdot \left[D_1 L_d(\boldsymbol{q}_n, \boldsymbol{q}_{n+1}) + D_2 L_d(\boldsymbol{q}_{n-1}, \boldsymbol{q}_n) + \boldsymbol{f}_{n-1}^+ + \boldsymbol{f}_n^- \right], \tag{3.14}$$

where

$$\boldsymbol{R}_d(\boldsymbol{q}_n) = \boldsymbol{G}_d^T(\boldsymbol{q}_n) \cdot \left(\boldsymbol{G}_d(\boldsymbol{q}_n) \cdot \boldsymbol{G}_d^T(\boldsymbol{q}_n) \right)^{-1}, \tag{3.15}$$

the following versions of the discrete Legendre transforms do not use Lagrange multipliers. The projected discrete Legendre transforms ${}^{Q}\mathbb{F}^{cf^-}L_d : Q \times Q \to \eta\left(T^*_{\boldsymbol{q}_n}C\right)$ and ${}^{Q}\mathbb{F}^{cf^+}L_d : Q \times Q \to \eta\left(T^*_{\boldsymbol{q}_n}C\right)$ read

$$\begin{aligned}
{}^{Q}\boldsymbol{p}_n^- &= \boldsymbol{Q}(\boldsymbol{q}_n) \cdot \left[-D_1 L_d(\boldsymbol{q}_n, \boldsymbol{q}_{n+1}) - \boldsymbol{f}_n^- \right] \\
{}^{Q}\boldsymbol{p}_n^+ &= \boldsymbol{Q}(\boldsymbol{q}_n) \cdot \left[D_2 L_d(\boldsymbol{q}_{n-1}, \boldsymbol{q}_n) + \boldsymbol{f}_{n-1}^+ \right],
\end{aligned} \tag{3.16}$$

where $\boldsymbol{Q}(\boldsymbol{q}_n)$ is given by

$$\boldsymbol{Q} = \boldsymbol{I}_{n\times n} - \boldsymbol{G}_d^T \cdot \left[\boldsymbol{G}_d \cdot \boldsymbol{M}^{-1} \cdot \boldsymbol{G}_d^T \right]^{-1} \boldsymbol{G}_d \cdot \boldsymbol{M}^{-1} \tag{3.17}$$

and fulfils $\boldsymbol{Q}(\boldsymbol{q}_n) \cdot \boldsymbol{G}_d^T(\boldsymbol{q}_n) = \boldsymbol{0}_{n\times m}$. Note that for the constrained discrete Legendre transforms and for the projected discrete Legendre transforms, the

output is an n-dimensional momentum vector. In the projected case, it lies in the $(n-m)$-dimensional submanifold $\eta\left(T^*_{\boldsymbol{q}_n}C\right)$ being the embedding of $T^*_{\boldsymbol{q}_n}C$ into $T^*_{\boldsymbol{q}_n}Q$. Yet another possibility is to compute an $(n-m)$-dimensional momentum vector by projecting with the discrete null space matrix. The reduced discrete Legendre transforms ${}^P\mathbb{F}^{cf^-}L_d : Q \times Q \to T^*U$ and ${}^P\mathbb{F}^{cf^+}L_d : Q \times Q \to T^*U$ are given by

$$\begin{aligned} {}^P\boldsymbol{p}_n^- &= \boldsymbol{P}^T(\boldsymbol{q}_n) \cdot \left[-D_1L_d(\boldsymbol{q}_n, \boldsymbol{q}_{n+1}) - \boldsymbol{f}_n^-\right] \\ {}^P\boldsymbol{p}_n^+ &= \boldsymbol{P}^T(\boldsymbol{q}_n) \cdot \left[D_2L_d(\boldsymbol{q}_{n-1}, \boldsymbol{q}_n) + \boldsymbol{f}_{n-1}^+\right]. \end{aligned} \tag{3.18}$$

This version is most appropriate to be used as a constraint in the optimisation problem, since it yields the minimal number of independent conditions, while conditions formulated using (3.16) are redundant and (3.13) involves the Lagrange multipliers.

Note that according to the range of the projection (3.17), ${}^Q\boldsymbol{p}_n$ fulfils the constraints on the momentum level; i.e.,

$$\boldsymbol{h}_d(\boldsymbol{q}_n, {}^Q\boldsymbol{p}_n) = \boldsymbol{G}(\boldsymbol{q}_n) \cdot \boldsymbol{M}^{-1} \cdot {}^Q\boldsymbol{p}_n = \boldsymbol{0} \tag{3.19}$$

while this is not in general the case for $\boldsymbol{p}_n$. This question is superfluous for ${}^P\boldsymbol{p}_n$.
Prescribed initial and final velocities of course should be consistent with the constraints on velocity level. Using the standard continuous Legendre transform $\mathbb{F}L : TC \to T^*C$

$$\mathbb{F}L : (\boldsymbol{q}, \dot{\boldsymbol{q}}) \mapsto (\boldsymbol{q}, \boldsymbol{p}) = (\boldsymbol{q}, D_2L(\boldsymbol{q}, \dot{\boldsymbol{q}})) \tag{3.20}$$

yields momenta which are consistent with the constraints on momentum level as well. With these preliminaries, the velocity boundary conditions are transformed to the following conditions on momentum level:

$$\boldsymbol{p}(t_0) = D_2L(\boldsymbol{q}(t_0), \dot{\boldsymbol{q}}(t_0)) = \boldsymbol{p}^0 \quad \text{and} \quad \boldsymbol{p}(t_N) = D_2L(\boldsymbol{q}(t_N), \dot{\boldsymbol{q}}(t_N)) = \boldsymbol{p}^N,$$

respectively. Then, $\boldsymbol{p}^0 = \boldsymbol{p}_0^-$ and $\boldsymbol{p}^N = \boldsymbol{p}_N^+$ are the corresponding conditions on the discrete level which read in detail

$$\begin{aligned} \boldsymbol{P}^T(\boldsymbol{q}_0) \cdot \left[D_2L(\boldsymbol{q}_0, \dot{\boldsymbol{q}}_0) + D_1L_d(\boldsymbol{q}_0, \boldsymbol{q}_1) + \boldsymbol{f}_0^-\right] &= \boldsymbol{0} \\ \boldsymbol{P}^T(\boldsymbol{q}_N) \cdot \left[D_2L(\boldsymbol{q}_N, \dot{\boldsymbol{q}}_N) - D_2L_d(\boldsymbol{q}_{N-1}, \boldsymbol{q}_N) - \boldsymbol{f}_{N-1}^+\right] &= \boldsymbol{0}. \end{aligned} \tag{3.21}$$

The Discrete Constrained Optimisation Problem. Now the optimal control problem for the constrained discrete motion can be formulated. To begin with, an approximation

$$B_d(\boldsymbol{q}_n, \boldsymbol{q}_{n+1}, \boldsymbol{f}_n) \approx \int_{t_n}^{t_{n+1}} B(\boldsymbol{q}, \dot{\boldsymbol{q}}, \boldsymbol{f})\, dt \tag{3.22}$$

of the continuous objective functional (2.2) has to be defined. As with the approximations (3.2), the midpoint rule is used:

$$B_d(\boldsymbol{q}_n, \boldsymbol{q}_{n+1}, \boldsymbol{f}_n) = hB\left(\frac{\boldsymbol{q}_{n+1}+\boldsymbol{q}_n}{2}, \frac{\boldsymbol{q}_{n+1}-\boldsymbol{q}_n}{h}, \boldsymbol{f}_n\right). \tag{3.23}$$

Jerry: Equations need punctuation throughout.	ToDo

This yields the discrete objective function

$$J_d(\boldsymbol{q}_d, \boldsymbol{f}_d) = \sum_{n=0}^{N-1} B_d(\boldsymbol{q}_n, \boldsymbol{q}_{n+1}, \boldsymbol{f}_n), \tag{3.24}$$

where the discrete configurations and forces are expressed in terms of their corresponding independent generalised quantities $\boldsymbol{u}_d = \{\boldsymbol{u}_n\}_{n=0}^{N}$ and $\boldsymbol{\tau}_d = \{\boldsymbol{\tau}_n\}_{n=0}^{N-1}$, respectively. Alternatively, a new objective function can be formulated directly in the generalised quantities

$$\bar{J}_d(\boldsymbol{u}_d, \boldsymbol{\tau}_d) = \sum_{n=0}^{N-1} \bar{B}_d(\boldsymbol{u}_n, \boldsymbol{u}_{n+1}, \boldsymbol{\tau}_n) \tag{3.25}$$

depending on the desired interpretation of the optimisation problem. In any case, (3.24) or (3.25) has to be minimised with respect to $\boldsymbol{u}_d, \boldsymbol{\tau}_d$ subject to the constraints

$$\begin{aligned}
\boldsymbol{u}_0 - \boldsymbol{u}^0 &= \boldsymbol{0} \\
\boldsymbol{D}(\boldsymbol{q}_N, \boldsymbol{q}^N) &= \boldsymbol{0} \\
\boldsymbol{P}^T(\boldsymbol{q}_0) \cdot \left[D_2 L(\boldsymbol{q}_0, \dot{\boldsymbol{q}}_0) + D_1 L_d(\boldsymbol{q}_0, \boldsymbol{q}_1) + \boldsymbol{f}_0^-\right] &= \boldsymbol{0} \\
\boldsymbol{P}^T(\boldsymbol{q}_N) \cdot \left[D_2 L(\boldsymbol{q}_N, \dot{\boldsymbol{q}}_N) - D_2 L_d(\boldsymbol{q}_{N-1}, \boldsymbol{q}_N) - \boldsymbol{f}_{N-1}^+\right] &= \boldsymbol{0} \\
\boldsymbol{P}^T(\boldsymbol{q}_n) \cdot \left[D_2 L_d(\boldsymbol{q}_{n-1}, \boldsymbol{q}_n) + D_1 L_d(\boldsymbol{q}_n, \boldsymbol{q}_{n+1}) + \boldsymbol{f}_{n-1}^+ + \boldsymbol{f}_n^-\right] &= \boldsymbol{0}
\end{aligned} \tag{3.26}$$

for $n = 1, \ldots, N-1$.

Remark 3.2 (Dimension of the constrained optimisation problem)**.** The use of the discrete null space method with nodal reparametrisation yields a constrained optimisation problem of minimal possible dimension: the optimisation of (3.24) or (3.25) subject to (3.26) includes $2N(n-m)$ variables and $(N+2)(n-m)$ constraints. In contrast to that, the optimisation problem resulting from the Lagrange multiplier formulation involves $N(2n+m)$ unknowns and $(N+2)(n+m)$ constraints (this are $3Nm$ more variables and $(N+2)2m$ more constraints). Of course, this influences the computational costs substantially.

4 Optimal Control for Rigid Body Dynamics

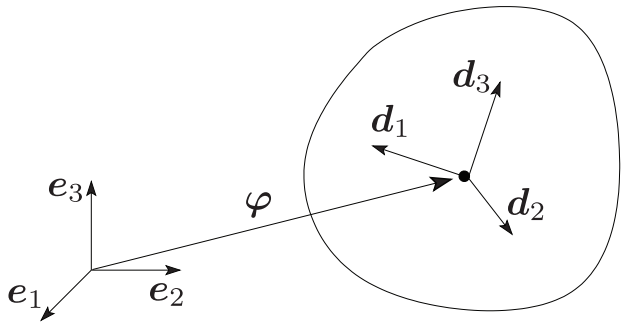

Figure 4.1: Configuration of a rigid body with respect to an orthonormal frame $\{e_I\}$ fixed in space.

Jerry: For me the picture needed to be rotated by 90 degrees, so I did that. One could also fix the original eps figures, but I do not have them, so could not do it that way. The font for the $\mathbf{d}_i$ in the figure does not match the text, where bold italic is used. Also, the ϕ in the figure is lightface, and in the text it is bold. In many other figures later on, the figure fonts do not match the text fonts.

ToDo

The treatment of rigid bodies as structural elements relies on the kinematic assumptions illustrated in Figure 4.1

A constrained formulation of rigid body dynamics (see Antmann [1995]; Betsch and Steinmann [2001]) is used in this work. The time-dependent configuration variable of a rigid body

$$\boldsymbol{q}(t) = \begin{bmatrix} \boldsymbol{\varphi}(t) \\ \boldsymbol{d}_1(t) \\ \boldsymbol{d}_2(t) \\ \boldsymbol{d}_3(t) \end{bmatrix} \in \mathbb{R}^{12} \tag{4.1}$$

consists of the placement of the centre of mass $\boldsymbol{\varphi} \in \mathbb{R}^3$ and the directors $\boldsymbol{d}_I \in \mathbb{R}^3, I = 1, 2, 3$ which are constrained to stay orthonormal during the motion, see Figure 4.1. Of course this is equivalent to specifying that the configuration manifold is the Euclidean group, SE(3), which is common in other treatments, such as Marsden and Ratiu [1999]. These constraints on the directors are called internal constraints, since they represent the underlying kinematic assumptions. Then the body's Euler tensor with respect to the

centre of mass can be related to the inertia tensor $\boldsymbol{J}$ via

$$\boldsymbol{E} = \frac{1}{2}(\mathrm{tr}\boldsymbol{J})\boldsymbol{I} - \boldsymbol{J}, \tag{4.2}$$

where $\boldsymbol{I}$ denotes the 3×3 identity matrix. The principal values of the Euler tensor E_i together with the body's total mass M_φ are ingredients in the rigid body's constant symmetric positive definite mass matrix

$$\boldsymbol{M} = \begin{bmatrix} M_\varphi \boldsymbol{I} & \boldsymbol{0} & \boldsymbol{0} & \boldsymbol{0} \\ \boldsymbol{0} & E_1 \boldsymbol{I} & \boldsymbol{0} & \boldsymbol{0} \\ \boldsymbol{0} & \boldsymbol{0} & E_2 \boldsymbol{I} & \boldsymbol{0} \\ \boldsymbol{0} & \boldsymbol{0} & \boldsymbol{0} & E_3 \boldsymbol{I} \end{bmatrix}, \tag{4.3}$$

where $\boldsymbol{0}$ denotes the 3×3 zero matrix.

The angular momentum of the rigid body can be computed as

$$\boldsymbol{L} = \boldsymbol{\varphi} \times \boldsymbol{p}_\varphi + \boldsymbol{d}_I \times \boldsymbol{p}_I, \tag{4.4}$$

where summation convention is used to sum over the repeated index I.

```
Jerry: Einstein's convention would have one index up and one
down.
```

ToDo

Null Space Matrix. An account of rigid body dynamics is given in Betsch and Leyendecker [2006]; Leyendecker [2006] where also the null space matrix

$$\boldsymbol{P}_{\mathrm{int}}(\boldsymbol{q}) = \begin{bmatrix} \boldsymbol{I} & \boldsymbol{0} \\ \boldsymbol{0} & -\widehat{\boldsymbol{d}_1} \\ \boldsymbol{0} & -\widehat{\boldsymbol{d}_2} \\ \boldsymbol{0} & -\widehat{\boldsymbol{d}_3} \end{bmatrix} \tag{4.5}$$

has been derived. Here $\widehat{\boldsymbol{a}}$ denotes the skew-symmetric 3×3 matrix with corresponding axial vector $\boldsymbol{a} \in \mathbb{R}^3$. For a single rigid body moving free in space, no external constraints are present, therefore $\boldsymbol{P}(\boldsymbol{q}) = \boldsymbol{P}_{\mathrm{int}}(\boldsymbol{q})$.

Nodal Reparametrisation. When the nodal reparametrisation of unknowns is applied, the configuration of the free rigid body is specified by six unknowns $\boldsymbol{u}_{n+1} = (\boldsymbol{u}_{\varphi_{n+1}}, \boldsymbol{\theta}_{n+1}) \in U \subset \mathbb{R}^3 \times \mathbb{R}^3$, characterising the incremental displacement and incremental rotation, respectively. Accordingly, in the present case the nodal reparametrisation $\boldsymbol{F} : U \times Q \to C$ introduced in (3.9) assumes the form

$$\boldsymbol{q}_{n+1} = \boldsymbol{F}_d(\boldsymbol{u}_{n+1}, \boldsymbol{q}_n) = \begin{bmatrix} \boldsymbol{\varphi}_n + \boldsymbol{u}_{\varphi_{n+1}} \\ \exp(\widehat{\boldsymbol{\theta}_{n+1}}) \cdot (\boldsymbol{d}_1)_n \\ \exp(\widehat{\boldsymbol{\theta}_{n+1}}) \cdot (\boldsymbol{d}_2)_n \\ \exp(\widehat{\boldsymbol{\theta}_{n+1}}) \cdot (\boldsymbol{d}_3)_n \end{bmatrix}, \tag{4.6}$$

where Rodrigues' formula is used to obtain a closed form expression of the exponential map, see e.g. Marsden and Ratiu [1999].

Actuation of the Rigid Body. Consider a single rigid body that is actuated by generalised forces

$$\boldsymbol{\tau}_{rb} = \begin{bmatrix} \boldsymbol{\tau}_\varphi \\ \boldsymbol{\tau}_\theta \end{bmatrix} \in \mathbb{R}^6 \tag{4.7}$$

consisting of a translational force $\boldsymbol{\tau}_\varphi \in \mathbb{R}^3$ and a torque $\boldsymbol{\tau}_\theta \in \mathbb{R}^3$. Assume that the force is not applied in the centre of mass, but in material points of the rigid body located at

$$\boldsymbol{\varrho}^{rb} = \varrho_I^{rb} \boldsymbol{d}_I \tag{4.8}$$

away from the centre of mass. This results in a force $\boldsymbol{\tau}_\varphi$ applied at the centre of mass and a torque $\boldsymbol{\varrho}^{rb} \times \boldsymbol{\tau}_\varphi + \boldsymbol{\tau}_\theta$ that are given by

$$\begin{bmatrix} \boldsymbol{\tau}_\varphi \\ \boldsymbol{\varrho}^{rb} \times \boldsymbol{\tau}_\varphi + \boldsymbol{\tau}_\theta \end{bmatrix} = \boldsymbol{C}_{rb}(\boldsymbol{q}) \cdot \boldsymbol{\tau}_{rb} \qquad \boldsymbol{C}_{rb}(\boldsymbol{q}) = \begin{bmatrix} \boldsymbol{I} & \boldsymbol{0} \\ \widehat{\boldsymbol{\varrho}}^{rb} & \boldsymbol{I} \end{bmatrix} \in \mathbb{R}^{6\times 6}. \tag{4.9}$$

As with (2.7), the redundant forces can be computed according to

$$\boldsymbol{f} = \begin{bmatrix} \boldsymbol{f}_\varphi \\ \boldsymbol{f}_1 \\ \boldsymbol{f}_2 \\ \boldsymbol{f}_3 \end{bmatrix} = \boldsymbol{B}^T(\boldsymbol{q}) \cdot \boldsymbol{\tau}_{rb} \in \mathbb{R}^{12}, \tag{4.10}$$

with

$$\boldsymbol{B}^T(\boldsymbol{q}) = \boldsymbol{P}_{\text{int}}(\boldsymbol{q}) \cdot \begin{bmatrix} \boldsymbol{I} & \boldsymbol{0} \\ \boldsymbol{0} & \frac{1}{2}\boldsymbol{I} \end{bmatrix} \cdot \boldsymbol{C}_{rb}(\boldsymbol{q}) \in \mathbb{R}^{12\times 6}. \tag{4.11}$$

A straightforward calculation shows

$$\boldsymbol{P}^T(\boldsymbol{q}) \cdot \boldsymbol{f} = \boldsymbol{C}_{rb}(\boldsymbol{q}) \cdot \boldsymbol{\tau}_{rb}. \tag{4.12}$$

The resulting reduced forces in (2.6) represent the effect of the applied forces and torques $\boldsymbol{\tau}_{rb}$ on the generalised degrees of freedom.

The same holds in the discrete setting, where the resulting reduced forces in (3.12)

$$\boldsymbol{P}^T(\boldsymbol{q}_n) \cdot (\boldsymbol{f}_{n-1}^+ + \boldsymbol{f}_n^-) = \boldsymbol{C}_{rb}(\boldsymbol{q}_n) \cdot \left(\boldsymbol{\tau}_{rb}{}_{n-1}^+ + \boldsymbol{\tau}_{rb}{}_n^-\right) \tag{4.13}$$

represent the effect of the applied forces and torques at t_n on the generalised degrees of freedom.

Proposition 4.1. *The above definition of the redundant left and right discrete forces guarantees that, in the absence of a potential energy, the change in angular momentum along the solution trajectory $\boldsymbol{q}_d$ of (3.12) is induced only by the effect of the discrete generalised forces.*

Proof. Computation of $\boldsymbol{p}_{n+1}^{+}$ and via $\boldsymbol{p}_{n}^{-}$ the discrete Legendre transforms (3.13) and insertion into the definition of angular momentum (4.4) yields

$$\begin{aligned}
&\boldsymbol{L}_{n+1} - \boldsymbol{L}_n \\
&\quad = \boldsymbol{\varphi}_{n+1} \times \boldsymbol{p}_{\varphi n+1}^{+} + \boldsymbol{d}_{In+1} \times \boldsymbol{p}_{In+1}^{+} - \boldsymbol{\varphi}_n \times \boldsymbol{p}_{\varphi n}^{-} - \boldsymbol{d}_{In} \times \boldsymbol{p}_{In}^{-} \\
&\quad = \boldsymbol{\varphi}_{n+1} \times \left(\boldsymbol{f}_{\varphi n}^{+}\right) + \boldsymbol{d}_{In+1} \times \left(\boldsymbol{f}_{In}^{+}\right) - \boldsymbol{\varphi}_n \times \left(-\boldsymbol{f}_{\varphi n}^{-}\right) - \boldsymbol{d}_{In} \times \left(-\boldsymbol{f}_{In}^{-}\right) \\
&\quad = \boldsymbol{\varphi}_{n+1} \times \boldsymbol{\tau}_{\varphi n}^{+} + \boldsymbol{d}_{In+1} \times \left(\frac{1}{2}\left(\boldsymbol{\varrho}_{n+1}^{rb} \times \boldsymbol{\tau}_{\varphi n}^{+} + \boldsymbol{\tau}_{\theta n}^{+}\right) \times \boldsymbol{d}_{In+1}\right) \qquad (4.14) \\
&\qquad + \boldsymbol{\varphi}_n \times \boldsymbol{\tau}_{\varphi n}^{-} + \boldsymbol{d}_{In} \times \left(\frac{1}{2}\left(\boldsymbol{\varrho}_{n}^{rb} \times \boldsymbol{\tau}_{\varphi n}^{-} + \boldsymbol{\tau}_{\theta n}^{-}\right) \times \boldsymbol{d}_{In}\right) \\
&\quad = \boldsymbol{\varphi}_{n+1} \times \boldsymbol{\tau}_{\varphi n}^{+} + \boldsymbol{\varrho}_{n+1}^{rb} \times \boldsymbol{\tau}_{\varphi n}^{+} + \boldsymbol{\tau}_{\theta n}^{+} + \boldsymbol{\varphi}_n \times \boldsymbol{\tau}_{\varphi n}^{-} + \boldsymbol{\varrho}_{n}^{rb} \times \boldsymbol{\tau}_{\varphi n}^{-} + \boldsymbol{\tau}_{\theta n}^{-}.
\end{aligned}$$

A straightforward calculation shows that all terms stemming from the kinetic energy and the constraint forces cancel. ■

Remark 4.2 (The Presence of Gravity)**.** The computation in (4.14) is performed for the case in which no potential energy is present. With an acceleration $g \in \mathbb{R}$ due to gravity in the negative $\boldsymbol{e}_3$-direction, the corresponding potential reads

$$V(\boldsymbol{q}) = \begin{bmatrix} 0 \\ 0 \\ -M_\varphi g \\ 0 \\ \vdots \\ 0 \end{bmatrix}^T \cdot \boldsymbol{q}. \qquad (4.15)$$

In this case, (4.14) yields

$$\begin{aligned}
\boldsymbol{L}_{n+1} - \boldsymbol{L}_n = \boldsymbol{\varphi}_{n+1} \times \boldsymbol{\tau}_{\varphi n}^{+} + \boldsymbol{\varrho}_{n+1}^{rb} \times \boldsymbol{\tau}_{\varphi n}^{+} + \boldsymbol{\tau}_{\theta n}^{+} + \boldsymbol{\varphi}_n \times \boldsymbol{\tau}_{\varphi n}^{-} + \boldsymbol{\varrho}_{n}^{rb} \times \boldsymbol{\tau}_{\varphi n}^{-} + \boldsymbol{\tau}_{\theta n}^{-} \\
- \left(\boldsymbol{\varphi}_{n+1} + \boldsymbol{\varphi}_n\right) \times \frac{h}{2} \begin{bmatrix} 0 \\ 0 \\ -M_\varphi g \end{bmatrix}, \qquad (4.16)
\end{aligned}$$

meaning that the third component of the angular momentum changes only according to the applied forces while the change in the first and second component is influenced by gravity as well. In particular in the absence of any external forces, this shows that the third component of the angular momentum is conserved exactly.

5 Optimal Control for Kinematic Pairs

The constrained formulation of the dynamics of kinematic pairs and the subsequent reduction of the equations of motion via the discrete null space method

with nodal reparametrisation has been introduced in Betsch and Leyendecker [2006]; Leyendecker [2006] for conservative systems. The main ingredients will be recalled here briefly. Furthermore it will be shown how the generalised forces of a kinematic pair act on the respective bodies.

Remark 5.1 (Comparisons with Betsch and Leyendecker [2006] and Leyendecker [2006])**.** The idea of this procedure was originally investigated in the framework of energy-momentum conserving time-integration of multibody dynamics in Betsch and Leyendecker [2006] and Leyendecker [2006]. However, a slightly different point of view is taken here: In a kinematic pair, the motion of the second body with respect to an **axis** fixed in the first body (or with respect to a plane for the planar pair) is represented by the joint velocities. This is in contrast to Betsch and Leyendecker [2006] and Leyendecker [2006], where joint velocities represent the relative motion of the second body with respect to the **first body**. If e.g. for a revolute pair, the first body performs rotation only about the axis of relative rotation, the second body performs the same rotation using the formulation of Betsch and Leyendecker [2006] and Leyendecker [2006], while it remains motionless with the new kinematic assumptions. The different interpretation of the motion of neighbouring bodies is explained for each joint connection in the respective section. Eventually, this different point of view leads to null space matrices and nodal reparametrisations that are slightly different from those given in Betsch and Leyendecker [2006] and Leyendecker [2006]. As a consequence, the resulting simulation tools for multibody dynamics can be extended to include actuating forces in an easier way.

The coupling of two neighbouring links (body 1 and body 2) by a specific joint J yields $m_{\text{ext}}^{(J)}$ external constraints $\boldsymbol{g}_{\text{ext}}(\boldsymbol{q}) \in \mathbb{R}^{m_{\text{ext}}^{(J)}}$ where the configuration variable

$$\boldsymbol{q} = \begin{bmatrix} \boldsymbol{q}^1 \\ \boldsymbol{q}^2 \end{bmatrix} \in \mathbb{R}^{24} \tag{5.1}$$

consists of $\boldsymbol{q}^\alpha, \alpha = 1, 2$ of the form (4.1). The 24×24 mass matrix of a kinematic pair consists of two blocks of the form (4.3). Here, $J \in \{R, P, C, S, E\}$, i.e. revolute, prismatic, cylindrical, spherical and planar couplings are considered. Depending on the number of external constraints $m_{\text{ext}}^{(J)}$ they give rise to, the degrees of freedom of the relative motion of one body with respect to the other is decreased from 6 to $r^{(J)} = 6 - m_{\text{ext}}^{(J)}$. The location of a specific joint in the α-th body is characterised by coordinates ϱ_i^α in the body frame $\{\boldsymbol{d}_I^\alpha\}$ for $\alpha = 1, 2$

$$\boldsymbol{\varrho}^\alpha = \varrho_i^\alpha \boldsymbol{d}_i^\alpha. \tag{5.2}$$

Null Space Matrix. The total null space matrix associated with a kinematic pair can be calculated from

$$\boldsymbol{P}^{(J)}(\boldsymbol{q}) = \begin{bmatrix} \boldsymbol{P}_{\text{int}}(\boldsymbol{q}^1) & \boldsymbol{0}_{12\times r^{(J)}} \\ \boldsymbol{P}_{\text{int}}(\boldsymbol{q}^2)\cdot\boldsymbol{P}^{2,(J)}_{\text{ext}}(\boldsymbol{q}) \end{bmatrix}, \tag{5.3}$$

where the internal null space matrix of each body is given in (4.5) and the $6\times(6+r^{(J)})$ matrix $\boldsymbol{P}^{2,(J)}_{\text{ext}}(\boldsymbol{q})$ accounts for the coupling induced by a specific joint.

Nodal Reparametrisation. The redundant coordinates $\boldsymbol{q}\in\mathbb{R}^{24}$ of each kinematic pair $J\in\{R,P,C,S,E\}$ may be expressed in terms of $6+r^{(J)}$ independent generalised coordinates. When using a reparametrisation of unknowns in the discrete null space method, relationships of the form

$$\boldsymbol{q}_{n+1} = \boldsymbol{F}^{(J)}(\boldsymbol{\mu}^{(J)}_{n+1}, \boldsymbol{q}_n) \tag{5.4}$$

are required, where

$$\boldsymbol{\mu}^{(J)}_{n+1} = (\boldsymbol{u}^1_{\varphi_{n+1}}, \boldsymbol{\theta}^1_{n+1}, \boldsymbol{\vartheta}^{(J)}_{n+1}) \in \mathbb{R}^{6+r^{(J)}} \tag{5.5}$$

consists of a minimal number of incremental unknowns in $[t_n, t_{n+1}]$ for a specific kinematic pair. In (5.5), $(\boldsymbol{u}^1_{\varphi_{n+1}}, \boldsymbol{\theta}^1_{n+1})\in\mathbb{R}^3\times\mathbb{R}^3$ are incremental displacements and rotations, respectively, associated with the first body (see Section 4). Furthermore, $\boldsymbol{\vartheta}^{(J)}_{n+1}\in\mathbb{R}^{r^{(J)}}$ denotes incremental unknowns which characterise the configuration of the second body relative to the axis (or plane in case of the E pair) of relative motion fixed in the first body. In view of (5.1), the mapping in (5.4) may be partitioned according to

$$\begin{aligned} \boldsymbol{q}^1_{n+1} &= \boldsymbol{F}^1(\boldsymbol{u}^1_{\varphi_{n+1}}, \boldsymbol{\theta}^1_{n+1}, \boldsymbol{q}^1_n) \\ \boldsymbol{q}^2_{n+1} &= \boldsymbol{F}^{2,(J)}(\boldsymbol{\mu}^{(J)}_{n+1}, \boldsymbol{q}_n), \end{aligned} \tag{5.6}$$

where $\boldsymbol{F}^1(\boldsymbol{u}^1_{\varphi_{n+1}}, \boldsymbol{\theta}^1_{n+1}, \boldsymbol{q}^1_n)$ is given by (4.6) and $\boldsymbol{F}^{2,(J)}(\boldsymbol{\mu}^{(J)}_{n+1}, \boldsymbol{q}_n)$ remains to be specified for each kinematic pair.

The null space matrices and nodal reparametrisations for the joints based on the new kinematic assumptions (see Remark 5.1) and in particular a consistent expression for the redundant forces that ensures consistency of momentum maps are given in §5.1—§5.5.

Actuation of a Kinematic Pair. The actuation of kinematic pairs is twofold. First of all, the overall motion of the pair can be influenced by applying translational forces and torques $\boldsymbol{\tau}_{rb}\in\mathbb{R}^6$ to one of the bodies, say

body 1. Any resulting change in the first bodies velocities will be transferred to the second body via the constrained equations of motion. Secondly, the relative motion of the pair can be influenced. Actuation of the joint connection itself by joint forces $\boldsymbol{\tau}^{(J)} \in \mathbb{R}^{r^{(J)}}$ effects both bodies, where according to "action equals reaction", the resulting generalised forces on the bodies are equal, but opposite in sign, see e.g. Bullo and Lewis [2004]. The dimension of the joint force $\boldsymbol{\tau}^{(J)}$ is determined by the number of relative degrees of freedom $r^{(J)}$ permitted by the specific joint.

Altogether, the generalised forces

$$\begin{bmatrix} \boldsymbol{\tau}_{rb} \\ \boldsymbol{\tau}^{(J)} \end{bmatrix} \in \mathbb{R}^{6+r^{(J)}} \tag{5.7}$$

act on the kinematic pair. The redundant forces can then be computed similar to (2.7) as

$$\boldsymbol{f} = \begin{bmatrix} \boldsymbol{f}^1 \\ \boldsymbol{f}^2 \end{bmatrix} = \boldsymbol{B}^T(\boldsymbol{q}) \cdot \begin{bmatrix} \boldsymbol{\tau}_{rb} \\ \boldsymbol{\tau}^{(J)} \end{bmatrix} \in \mathbb{R}^{24}, \tag{5.8}$$

with the $24 \times (6 + r^{(J)})$ matrix

$$\boldsymbol{B}^T(\boldsymbol{q}) = \begin{bmatrix} \boldsymbol{P}_{\text{int}}(\boldsymbol{q}^1) & \boldsymbol{0} \\ \boldsymbol{0} & \boldsymbol{P}_{\text{int}}(\boldsymbol{q}^2) \end{bmatrix} \cdot \begin{bmatrix} \boldsymbol{I} & \boldsymbol{0} & \boldsymbol{0} & \boldsymbol{0} \\ \boldsymbol{0} & \frac{1}{2}\boldsymbol{I} & \boldsymbol{0} & \boldsymbol{0} \\ \boldsymbol{0} & \boldsymbol{0} & \boldsymbol{I} & \boldsymbol{0} \\ \boldsymbol{0} & \boldsymbol{0} & \boldsymbol{0} & \frac{1}{2}\boldsymbol{I} \end{bmatrix} \cdot \begin{bmatrix} \boldsymbol{C}_{rb}(\boldsymbol{q}^1) & \boldsymbol{C}^{1,(J)}(\boldsymbol{q}) \\ \boldsymbol{0} & \boldsymbol{C}^{2,(J)}(\boldsymbol{q}) \end{bmatrix} \tag{5.9}$$

and the $6 \times r^{(J)}$ matrices $\boldsymbol{C}^{\alpha,(J)}(\boldsymbol{q}), \alpha = 1, 2$ being specified according to the specific joint in use.

As with equation (4.12), the product of the transposed null space matrix and the redundant forces yields the effect of the generalised forces on the generalised degrees of freedom of the kinematic pair. The corresponding expression of the actuation is given for each kinematic pair in the sequel.

5.1 Spherical Pair

Constraints. The S pair (Figure 5.1) prevents all relative translation between the two bodies, thus it entails three external constraints of the form

$$\boldsymbol{g}_{\text{ext}}^{(S)}(\boldsymbol{q}) = \boldsymbol{\varphi}^2 - \boldsymbol{\varphi}^1 + \boldsymbol{\varrho}^2 - \boldsymbol{\varrho}^1 = \boldsymbol{0}. \tag{5.10}$$

The corresponding independent velocities are the first body's translational velocity $\dot{\boldsymbol{\varphi}}^1$ and angular velocity $\boldsymbol{\omega}^1$ and the second body's angular velocity $\boldsymbol{\omega}^2$.

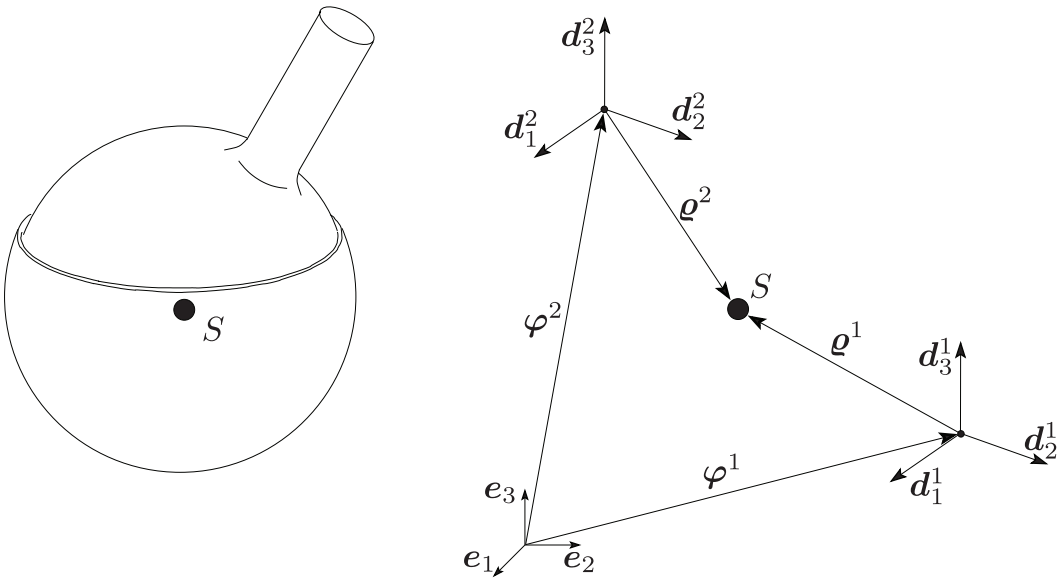

Figure 5.1: Spherical pair.

Null Space Matrix. The null space matrix for the S pair follows directly from (5.3) with

$$\boldsymbol{P}_{\text{int}}(\boldsymbol{q}^2) \cdot \boldsymbol{P}_{\text{ext}}^{2,(S)}(\boldsymbol{q}) = \begin{bmatrix} \boldsymbol{I} & -\widehat{\boldsymbol{\varrho}^1} & \widehat{\boldsymbol{\varrho}^2} \\ \boldsymbol{0} & \boldsymbol{0} & -\widehat{\boldsymbol{d}_1^2} \\ \boldsymbol{0} & \boldsymbol{0} & -\widehat{\boldsymbol{d}_2^2} \\ \boldsymbol{0} & \boldsymbol{0} & -\widehat{\boldsymbol{d}_3^2} \end{bmatrix}. \tag{5.11}$$

Nodal Reparametrisation. In the reduced set of incremental unknowns (5.5) for the S pair, $\boldsymbol{\vartheta}_{n+1}^{(S)} = \boldsymbol{\theta}_{n+1}^2 \in \mathbb{R}^3$ represents the incremental rotation vector pertaining to the second body. Then the mapping in $(5.6)_2$ reads

$$\boldsymbol{q}_{n+1}^2 = \boldsymbol{F}^{2,(S)}(\boldsymbol{\mu}_{n+1}^{(S)}, \boldsymbol{q}_n) = \begin{bmatrix} \boldsymbol{\varphi}_n^1 + \boldsymbol{u}_{\varphi_{n+1}}^1 + \exp(\widehat{\boldsymbol{\theta}_{n+1}^1}) \cdot \boldsymbol{\varrho}_n^1 - \exp(\widehat{\boldsymbol{\theta}_{n+1}^2}) \cdot \boldsymbol{\varrho}_n^2 \\ \exp(\widehat{\boldsymbol{\theta}_{n+1}^2}) \cdot (\boldsymbol{d}_1^2)_n \\ \exp(\widehat{\boldsymbol{\theta}_{n+1}^2}) \cdot (\boldsymbol{d}_2^2)_n \\ \exp(\widehat{\boldsymbol{\theta}_{n+1}^2}) \cdot (\boldsymbol{d}_3^2)_n \end{bmatrix}. \tag{5.12}$$

The null space matrix and nodal reparametrisation for the S pair do not differ from those given in Betsch and Leyendecker [2006]; Leyendecker [2006].

Actuation of the Spherical Pair. A torque $\boldsymbol{\tau}^{(S)} \in \mathbb{R}^3$ can be applied at the spherical joint. Then the forces on each body are computed according to

(5.8) with

$$\boldsymbol{C}^{1,(S)}(\boldsymbol{q}) = \begin{bmatrix} \boldsymbol{0} \\ -\boldsymbol{I} \end{bmatrix} \qquad \boldsymbol{C}^{2,(S)}(\boldsymbol{q}) = \begin{bmatrix} \boldsymbol{0} \\ \boldsymbol{I} \end{bmatrix}. \tag{5.13}$$

The generalised forces effect the following actuation of the generalised degrees of freedom of the spherical pair. In addition to the rigid body actuation, the first body's rotation is influenced by the joint torque, which also actuates the relative rotation of the second body.

$$\left(\boldsymbol{P}^{(S)}(\boldsymbol{q})\right)^T \cdot \boldsymbol{f} = \begin{bmatrix} \boldsymbol{\tau}_\varphi \\ \boldsymbol{\varrho}^{rb} \times \boldsymbol{\tau}_\varphi + \boldsymbol{\tau}_\theta - \boldsymbol{\tau}^{(S)} \\ \boldsymbol{\tau}^{(S)} \end{bmatrix} \tag{5.14}$$

Proposition 5.2. *This definition of the redundant left and right discrete forces guarantees that the change of angular momentum along the solution trajectory $\boldsymbol{q}_d$ of (3.12) is induced only by the effect of the discrete generalised forces $\boldsymbol{\tau}_{rb}$. In particular, it is conserved exactly, if the motion of the pair is induced by shape changes only.*

Proof. In proving the second statement, it is assumed that only the joint is actuated, i.e. $\boldsymbol{\tau}_{rb} = \boldsymbol{0}$. Computation of $\boldsymbol{p}_{n+1}^+$ and via $\boldsymbol{p}_n^-$ the discrete Legendre transform (3.13) and insertion into the definition of angular momentum (4.4) yields

$$\begin{aligned}
&\boldsymbol{L}_{n+1} - \boldsymbol{L}_n \\
&\quad = \boldsymbol{\varphi}_{n+1}^1 \times \boldsymbol{p}_{\varphi_{n+1}}^{1\,+} + \boldsymbol{d}_{I\,n+1}^1 \times \boldsymbol{p}_{I\,n+1}^{1+} + \boldsymbol{\varphi}_{n+1}^2 \times \boldsymbol{p}_{\varphi_{n+1}}^{2\,+} + \boldsymbol{d}_{I\,n+1}^2 \times \boldsymbol{p}_{I\,n+1}^{2+} + \\
&\qquad - \boldsymbol{\varphi}_n^1 \times \boldsymbol{p}_{\varphi_n}^{1\,-} - \boldsymbol{d}_{I\,n}^1 \times \boldsymbol{p}_{I\,n}^{1-} - \boldsymbol{\varphi}_n^2 \times \boldsymbol{p}_{\varphi_n}^{2\,-} - \boldsymbol{d}_{I\,n}^2 \times \boldsymbol{p}_{I\,n}^{2-} \\
&\quad = \boldsymbol{d}_{I\,n+1}^1 \times \left(-\frac{1}{2}\boldsymbol{\tau}_n^{(S)^+} \times \boldsymbol{d}_{I\,n+1}^1\right) + \boldsymbol{d}_{I\,n+1}^2 \times \left(\frac{1}{2}\boldsymbol{\tau}_n^{(S)^+} \times \boldsymbol{d}_{I\,n+1}^2\right) + \\
&\qquad \boldsymbol{d}_{I\,n}^1 \times \left(-\frac{1}{2}\boldsymbol{\tau}_n^{(S)^-} \times \boldsymbol{d}_{I\,n}^1\right) + \boldsymbol{d}_{I\,n}^2 \times \left(\frac{1}{2}\boldsymbol{\tau}_n^{(S)^-} \times \boldsymbol{d}_{I\,n}^2\right) \\
&\quad = -\boldsymbol{\tau}_n^{(S)^+} + \boldsymbol{\tau}_n^{(S)^+} - \boldsymbol{\tau}_n^{(S)^-} + \boldsymbol{\tau}_n^{(S)^-} = \boldsymbol{0}.
\end{aligned} \tag{5.15}$$

The first statement follows by combining (5.15) and (4.14). ■

Jerry: Prefer setting this display like that in (4.14)	ToDo

5.2 Cylindrical pair

For the C pair (Figure 5.2), a unit vector $\boldsymbol{n}^1$ is introduced which is fixed in the first body and specified by constant components n_I^1 with respect to the body

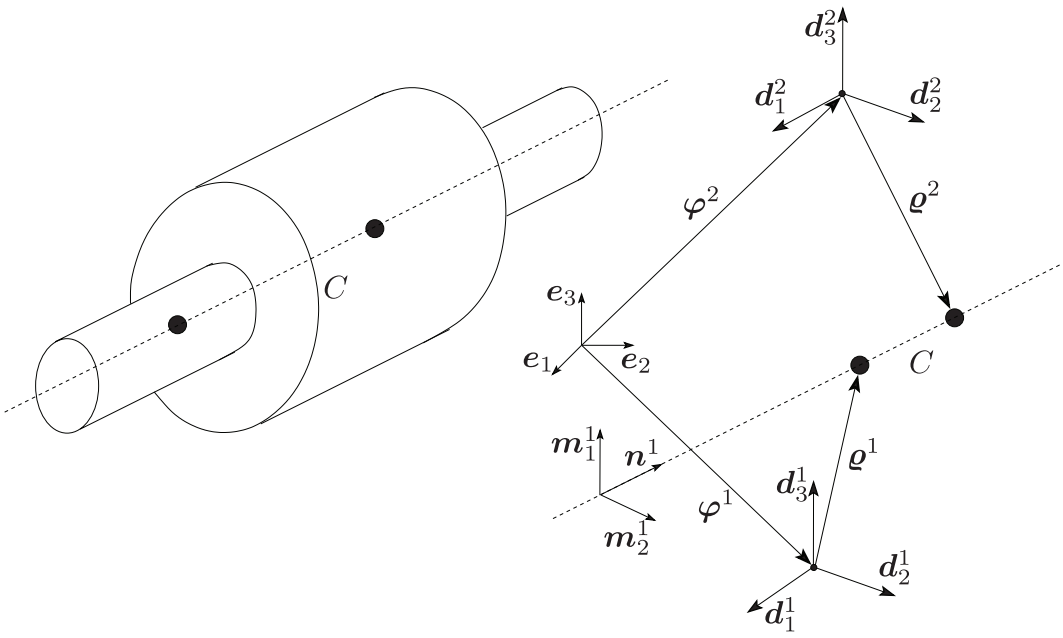

Figure 5.2: Cylindrical pair.

frame $\{\boldsymbol{d}_I^1\}$

$$\boldsymbol{n}^1 = n_I^1 \boldsymbol{d}_I^1. \tag{5.16}$$

In addition to that for $\kappa = 1, 2$, two vectors

$$\boldsymbol{m}_\kappa^1 = (m_\kappa^1)_I \boldsymbol{d}_I^1 \tag{5.17}$$

are introduced such that $\{\boldsymbol{m}_1^1, \boldsymbol{m}_2^1, \boldsymbol{n}^1\}$ constitute a right-handed orthonormal frame. The motion of the second body relative to the axis $\boldsymbol{n}^1$ can be described by $r^{(C)} = 2$ degrees of freedom: translation along $\boldsymbol{n}^1$ and rotation about $\boldsymbol{n}^1$. The translational motion along $\boldsymbol{n}^1$ may be characterised by the displacement $u^2 \in \mathbb{R}$, such that

$$\boldsymbol{\varphi}^1 + \boldsymbol{\varrho}^1 + u^2 \boldsymbol{n}^1 = \boldsymbol{\varphi}^2 + \boldsymbol{\varrho}^2. \tag{5.18}$$

For the subsequent treatment it proves convenient to introduce the vectors

$$\boldsymbol{s}^\alpha = \boldsymbol{\varphi}^\alpha + \boldsymbol{\varrho}^\alpha \tag{5.19}$$

for $\alpha = 1, 2$.

Constraints. The C pair entails $m_{\text{ext}}^{(C)} = 4$ external constraint functions that may be written in the form

$$\boldsymbol{g}_{\text{ext}}^{(C)}(\boldsymbol{q}) = \begin{bmatrix} (\boldsymbol{m}_1^1)^T \cdot (\boldsymbol{s}^2 - \boldsymbol{s}^1) \\ (\boldsymbol{m}_2^1)^T \cdot (\boldsymbol{s}^2 - \boldsymbol{s}^1) \\ (\boldsymbol{n}^1)^T \cdot \boldsymbol{d}_1^2 - \eta_1 \\ (\boldsymbol{n}^1)^T \cdot \boldsymbol{d}_2^2 - \eta_2 \end{bmatrix}, \tag{5.20}$$

where η_1, η_2 are constant and need be consistent with the initial conditions. Besides being influenced by the independent velocities of the first body, the second body's motion is characterised by $\dot{u}^2, \dot{\theta}^2$, where, in addition to u^2 already introduced in (5.18), $\dot{\theta}^2$ accounts for the angular velocity of the second body relative to $\boldsymbol{n}^1$.

Remark 5.3 (Comparison with Betsch and Leyendecker [2006]; Leyendecker [2006])**.** The assumption

$$\boldsymbol{\omega}^2 = \boldsymbol{\omega}^1 + \dot{\theta}^2 \boldsymbol{n}^1 \tag{5.21}$$

used in Betsch and Leyendecker [2006]; Leyendecker [2006] induces the second body to perform the same rotational motion as the first one and to additionally rotate relative to it about the axis $\boldsymbol{n}^1$. In particular, the second body follows the first bodies rotation about $\boldsymbol{n}^1$ if the relative velocity is zero. For example a pure rotation of the first body about $\boldsymbol{n}^1$ would affect the second body, but not vice versa according to (5.21). The new kinematic assumptions to be introduced in (5.22) and (5.23) in combination with the new update formula (5.25) completely decouple the bodies with respect to rotations about and translations along $\boldsymbol{n}^1$. Therefore it is easier to apply joint actuations that lead to momentum consistent dynamics.

```
Jerry:  Above paragraph has forward references, which should
be avoided.  Or, instead of ‘‘The new kinematic assumptions
(5.22)", say ‘‘The new kinematic assumptions to be introduced
in (5.22)’’, etc.
```

ToDo

Null Space Matrix. Specifically, the new relation between the angular velocities reads

$$\boldsymbol{\omega}^2 = \boldsymbol{I}^{11} \cdot \boldsymbol{\omega}^1 + \dot{\theta}^2 \boldsymbol{n}^1. \tag{5.22}$$

It ensures that the translation along and rotation about the axis $\boldsymbol{n}^1$ of one body leaves the other body motionless.

Differentiating (5.18) with respect to time and taking into account (5.22) and the assumption that a pure translation of body one along the axis of relative translation $\boldsymbol{n}^1$ should not affect body two, yields

$$\dot{\boldsymbol{\varphi}}^2 = \boldsymbol{I}^{11} \cdot \dot{\boldsymbol{\varphi}}^1 + \boldsymbol{\omega}^1 \times (\boldsymbol{\varrho}^1 + u^2 \boldsymbol{n}^1) - \left[\boldsymbol{I}^{11} \cdot \boldsymbol{\omega}^1\right] \times \boldsymbol{\varrho}^2 + \dot{u}^2 \boldsymbol{n}^1 + \dot{\theta}^2 \boldsymbol{\varrho}^2 \times \boldsymbol{n}^1, \tag{5.23}$$

where $\boldsymbol{I}^{11} = \boldsymbol{I} - \boldsymbol{n}^1 \otimes \boldsymbol{n}^1$. The null space matrix for the C pair can be inferred

from (5.3) with

$$\boldsymbol{P}_{\text{int}}(\boldsymbol{q}^2)\cdot\boldsymbol{P}^{2,(C)}_{\text{ext}}(\boldsymbol{q}) = \begin{bmatrix} \boldsymbol{I}^{11} & \widehat{\boldsymbol{\varrho}^2}\cdot\boldsymbol{I}^{11} - \widehat{\boldsymbol{\varrho}^1} - \widehat{u^2\boldsymbol{n}^1} & \boldsymbol{n}^1 & \boldsymbol{\varrho}^2\times\boldsymbol{n}^1 \\ \boldsymbol{0} & -\widehat{\boldsymbol{d}^2_1}\cdot\boldsymbol{I}^{11} & \boldsymbol{0} & \boldsymbol{n}^1\times\boldsymbol{d}^2_1 \\ \boldsymbol{0} & -\widehat{\boldsymbol{d}^2_2}\cdot\boldsymbol{I}^{11} & \boldsymbol{0} & \boldsymbol{n}^1\times\boldsymbol{d}^2_2 \\ \boldsymbol{0} & -\widehat{\boldsymbol{d}^2_3}\cdot\boldsymbol{I}^{11} & \boldsymbol{0} & \boldsymbol{n}^1\times\boldsymbol{d}^2_3 \end{bmatrix}. \tag{5.24}$$

Nodal Reparametrisation. For the C pair, the configuration of the second body with respect to the axis $\boldsymbol{n}^1$ can be characterised by $\boldsymbol{\vartheta}^{(C)}_{n+1} = (u^2_{n+1}, \theta^2_{n+1}) \in \mathbb{R}^2$. Here θ^2_{n+1} accounts for the incremental rotation. The rotation of the second body's directors consist of this rotation and that part of the rotation of body one which is not about the axis $\boldsymbol{n}^1$. Using the notation

$$\boldsymbol{R}^{1,2} = \exp(\widehat{\boldsymbol{\theta}^1_{n+1}})\cdot\exp(-\widehat{(\boldsymbol{n}^1_n\otimes\boldsymbol{n}^1_n)\cdot\boldsymbol{\theta}^1_{n+1}}),$$

it may be expressed via the product of exponentials formula

$$\boldsymbol{q}^2_{n+1} = \boldsymbol{F}^{2,(C)}(\boldsymbol{\mu}^{(C)}_{n+1}, \boldsymbol{q}_n) = \begin{bmatrix} \boldsymbol{\varphi}^1_n + \boldsymbol{I}^{11}_n\cdot\boldsymbol{u}^1_{\varphi_{n+1}} + \exp(\widehat{\boldsymbol{\theta}^1_{n+1}})\cdot[\boldsymbol{\varrho}^1_n + (\bar{u}^2_n + u^2_{n+1})\boldsymbol{n}^1_n] - \boldsymbol{R}^{1,2}\cdot\exp\left(\theta^2_{n+1}\widehat{\boldsymbol{n}^1_n}\right)\cdot\boldsymbol{\varrho}^2_n \\ \boldsymbol{R}^{1,2}\cdot\exp\left(\theta^2_{n+1}\widehat{\boldsymbol{n}^1_n}\right)\cdot(\boldsymbol{d}^2_1)_n \\ \boldsymbol{R}^{1,2}\cdot\exp\left(\theta^2_{n+1}\widehat{\boldsymbol{n}^1_n}\right)\cdot(\boldsymbol{d}^2_2)_n \\ \boldsymbol{R}^{1,2}\cdot\exp\left(\theta^2_{n+1}\widehat{\boldsymbol{n}^1_n}\right)\cdot(\boldsymbol{d}^2_3)_n \end{bmatrix}, \tag{5.25}$$

where $\boldsymbol{I}^{11}_n = \boldsymbol{I} - \boldsymbol{n}^1_n\otimes\boldsymbol{n}^1_n$ and $\bar{u}^2_n = \boldsymbol{n}^1_n\cdot(\boldsymbol{s}^2_n - \boldsymbol{s}^1_n)$ denotes the translation of the second body relative to the first one in the direction of the axis $\boldsymbol{n}^1_n$ at time t_n.

Actuation of the cylindrical pair The two relative degrees of freedom allowed by the cylindrical joint can be actuated by a translational force $\tau^{(C)}_\varphi \in \mathbb{R}$ that acts in the direction of the axis $\boldsymbol{n}^1$ and a torque $\tau^{(C)}_\theta \in \mathbb{R}$ about $\boldsymbol{n}^1$. Even if the joint is located away from the centres of mass, translational force along $\boldsymbol{n}^1$ can not cause a relative rotation of the second body for this pair. However, it causes the pair to rotate according to a torque $(\boldsymbol{\varphi}^1 - \boldsymbol{\varphi}^2)\times\boldsymbol{n}^1$, which is assigned to the first body. Using the matrices

$$\boldsymbol{C}^{1,(C)}(\boldsymbol{q}) = \begin{bmatrix} -\boldsymbol{n}^1 & \boldsymbol{0} \\ (\boldsymbol{\varphi}^1 - \boldsymbol{\varphi}^2)\times\boldsymbol{n}^1 & -\boldsymbol{n}^1 \end{bmatrix} \qquad \boldsymbol{C}^{2,(C)}(\boldsymbol{q}) = \begin{bmatrix} \boldsymbol{n}^1 & \boldsymbol{0} \\ \boldsymbol{0} & \boldsymbol{n}^1 \end{bmatrix}, \tag{5.26}$$

consistent forces can be computed from (5.8). The actuation of the generalised degrees of freedom reads

$$\left(\boldsymbol{P}^{(C)}(\boldsymbol{q})\right)^T \cdot \boldsymbol{f} = \begin{bmatrix} \boldsymbol{\tau}_\varphi - \tau_\varphi^{(C)} \boldsymbol{n}^1 \\ \boldsymbol{\varrho}^{rb} \times \boldsymbol{\tau}_\varphi + \boldsymbol{\tau}_\theta - \tau_\theta^{(C)} \boldsymbol{n}^1 \\ \tau_\varphi^{(C)} \\ \tau_\theta^{(C)} \end{bmatrix}. \tag{5.27}$$

Note that the torque induced by a translational joint force $\tau_\varphi^{(C)}$ away from the centre of mass does not show up here, since the corresponding rotation is automatically determined by the solution of the coupled dynamical system.

Proposition 5.4. *This definition of the redundant left and right discrete forces guarantees that the change of angular momentum along the solution trajectory $\boldsymbol{q}_d$ of (3.12) is induced only by the effect of the discrete generalised forces $\boldsymbol{\tau}_{rb}$. In particular, it is conserved exactly, if the motion of the pair is induced by shape changes only.*

Proof. For proving the second statement, it is assumed that only the joint is actuated, i.e. $\boldsymbol{\tau}_{rb} = \boldsymbol{0}$ and computing $\boldsymbol{p}_{n+1}^+$ and via $\boldsymbol{p}_n^-$ the discrete Legendre transforms (3.13), the definition of angular momentum (4.4) yields

$$\begin{aligned}
&\boldsymbol{L}_{n+1} - \boldsymbol{L}_n \\
&\quad = \boldsymbol{\varphi}_{n+1}^1 \times \boldsymbol{p}_{\varphi_{n+1}}^{1\,+} + \boldsymbol{d}_{In+1}^1 \times \boldsymbol{p}_{In+1}^{1+} + \boldsymbol{\varphi}_{n+1}^2 \times \boldsymbol{p}_{\varphi_{n+1}}^{2\,+} + \boldsymbol{d}_{In+1}^2 \times \boldsymbol{p}_{In+1}^{2+} + \\
&\qquad - \boldsymbol{\varphi}_n^1 \times \boldsymbol{p}_{\varphi_n}^{1\,-} - \boldsymbol{d}_{In}^1 \times \boldsymbol{p}_{In}^{1-} - \boldsymbol{\varphi}_n^2 \times \boldsymbol{p}_{\varphi_n}^{2\,-} - \boldsymbol{d}_{In}^2 \times \boldsymbol{p}_{In}^{2-} \\
&\quad = \boldsymbol{\varphi}_{n+1}^1 \times \left(-\frac{h}{2} \tau_{\varphi_n}^{(C)} \boldsymbol{n}_{n+1}^1 \right) + \\
&\qquad \boldsymbol{d}_{In+1}^1 \times \left(-\frac{h}{4} \left(\tau_{\theta_n}^{(C)} \boldsymbol{n}_{n+1}^1 + \left(\boldsymbol{\varphi}_{n+1}^2 - \boldsymbol{\varphi}_{n+1}^1 \right) \times \tau_{\varphi_n}^{(C)} \boldsymbol{n}_{n+1}^1 \right) \times \boldsymbol{d}_{In+1}^1 \right) + \\
&\qquad \boldsymbol{\varphi}_{n+1}^2 \times \left(\frac{h}{2} \tau_{\varphi_n}^{(C)} \boldsymbol{n}_{n+1}^1 \right) + \boldsymbol{d}_{In+1}^2 \times \left(\frac{h}{4} \left(\tau_{\theta_n}^{(C)} \boldsymbol{n}_{n+1}^1 \right) \times \boldsymbol{d}_{In+1}^2 \right) + \\
&\qquad \boldsymbol{\varphi}_n^1 \times \left(-\frac{h}{2} \tau_{\varphi_n}^{(C)} \boldsymbol{n}_n^1 \right) + \boldsymbol{d}_{In}^1 \times \left(-\frac{h}{4} \left(\tau_{\theta_n}^{(C)} \boldsymbol{n}_n^1 + \left(\boldsymbol{\varphi}_n^2 - \boldsymbol{\varphi}_n^1 \right) \times \tau_{\varphi_n}^{(C)} \boldsymbol{n}_n^1 \right) \times \boldsymbol{d}_{In}^1 \right) + \\
&\qquad \boldsymbol{\varphi}_n^2 \times \left(\frac{h}{2} \tau_{\varphi_n}^{(C)} \boldsymbol{n}_n^1 \right) + \boldsymbol{d}_{In}^2 \times \left(\frac{h}{4} \left(\tau_{\theta_n}^{(C)} \boldsymbol{n}_n^1 \right) \times \boldsymbol{d}_{In}^2 \right) \\
&\quad = \frac{h}{2} \tau_{\varphi_n}^{(C)} \boldsymbol{n}_{n+1}^1 \times \left(\boldsymbol{\varphi}_{n+1}^1 - \boldsymbol{\varphi}_{n+1}^2 + \boldsymbol{\varphi}_{n+1}^2 - \boldsymbol{\varphi}_{n+1}^1 \right) + \\
&\qquad \frac{h}{2} \tau_{\varphi_n}^{(C)} \boldsymbol{n}_n^1 \times \left(\boldsymbol{\varphi}_n^1 - \boldsymbol{\varphi}_n^2 + \boldsymbol{\varphi}_n^2 - \boldsymbol{\varphi}_n^1 \right) + \\
&\qquad \frac{h}{2} \left(-\tau_{\theta_n}^{(C)} \boldsymbol{n}_{n+1}^1 + \tau_{\theta_n}^{(C)} \boldsymbol{n}_{n+1}^1 - \tau_{\theta_n}^{(C)} \boldsymbol{n}_n^1 + \tau_{\theta_n}^{(C)} \boldsymbol{n}_n^1 \right) = \boldsymbol{0}.
\end{aligned} \tag{5.28}$$

The first statement follows by combining (5.48) and (4.14). ■

Jerry: Above display should be reset, as with (4.14). ToDo

5.3 Revolute pair

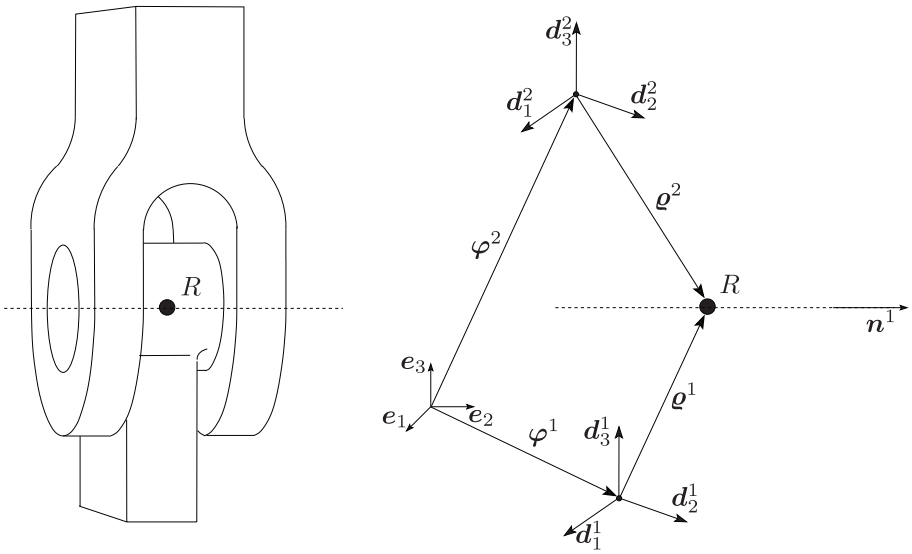

Figure 5.3: Revolute pair.

As for the cylindrical pair, use is made of the unit vector $\boldsymbol{n}^1$ given by (5.16), which specifies the axis of rotation of the second body relative to the first one.

Constraints. The R pair (Figure 5.3) entails $m_{\text{ext}}^{(R)} = 5$ external constraint functions which may be written in the form

$$\boldsymbol{g}_{\text{ext}}^{(R)}(\boldsymbol{q}) = \begin{bmatrix} \boldsymbol{\varphi}^2 - \boldsymbol{\varphi}^1 + \boldsymbol{\varrho}^2 - \boldsymbol{\varrho}^1 \\ (\boldsymbol{n}^1)^T \cdot \boldsymbol{d}_1^2 - \eta_1 \\ (\boldsymbol{n}^1)^T \cdot \boldsymbol{d}_2^2 - \eta_2 \end{bmatrix}. \tag{5.29}$$

Analogous to the cylindrical pair η_1, η_2 are constant and need be consistent with the initial conditions.

Null Space Matrix. The null space matrix for the R pair can directly be inferred from the previous treatment of the cylindrical pair where the column in the null space of the C pair associated with $\dot{u}^2$ has to be eliminated, as follows

$$\boldsymbol{P}_{\text{int}}^2(\boldsymbol{q}) \cdot \boldsymbol{P}_{\text{ext}}^{2,(R)}(\boldsymbol{q}) = \begin{bmatrix} \boldsymbol{I} & \widehat{\boldsymbol{\varrho}^2} \cdot \boldsymbol{I}^{11} - \widehat{\boldsymbol{\varrho}^1} & \boldsymbol{\varrho}^2 \times \boldsymbol{n}^1 \\ \boldsymbol{0} & -\widehat{\boldsymbol{d}_1^2} \cdot \boldsymbol{I}^{11} & \boldsymbol{n}^1 \times \boldsymbol{d}_1^2 \\ \boldsymbol{0} & -\widehat{\boldsymbol{d}_2^2} \cdot \boldsymbol{I}^{11} & \boldsymbol{n}^1 \times \boldsymbol{d}_2^2 \\ \boldsymbol{0} & -\widehat{\boldsymbol{d}_3^2} \cdot \boldsymbol{I}^{11} & \boldsymbol{n}^1 \times \boldsymbol{d}_3^2 \end{bmatrix}. \tag{5.30}$$

Nodal Reparametrisation. For the R pair the mapping $\boldsymbol{F}^{2,(R)}(\boldsymbol{\mu}^{(R)}_{n+1}, \boldsymbol{q}_n)$ can be directly obtained from that of the C pair by fixing $u^2_{n+1} = 0$.

$$\begin{aligned}\boldsymbol{q}^2_{n+1} &= \boldsymbol{F}^{2,(R)}(\boldsymbol{\mu}^{(R)}_{n+1}, \boldsymbol{q}_n) \\ &= \begin{bmatrix} \boldsymbol{\varphi}^1_n + \boldsymbol{u}^1_{\varphi_{n+1}} + \exp(\widehat{\boldsymbol{\theta}^1_{n+1}}) \cdot \boldsymbol{\varrho}^1_n - \boldsymbol{R}^{1,2} \cdot \exp\left(\theta^2_{n+1}\widehat{\boldsymbol{n}^1_n}\right) \cdot \boldsymbol{\varrho}^2_n \\ \boldsymbol{R}^{1,2} \cdot \exp\left(\theta^2_{n+1}\widehat{\boldsymbol{n}^1_n}\right) \cdot (\boldsymbol{d}^2_1)_n \\ \boldsymbol{R}^{1,2} \cdot \exp\left(\theta^2_{n+1}\widehat{\boldsymbol{n}^1_n}\right) \cdot (\boldsymbol{d}^2_2)_n \\ \boldsymbol{R}^{1,2} \cdot \exp\left(\theta^2_{n+1}\widehat{\boldsymbol{n}^1_n}\right) \cdot (\boldsymbol{d}^2_3)_n \end{bmatrix}\end{aligned} \tag{5.31}$$

Jerry: Prededing equation is too wide. ToDo

Actuation of the Revolute Pair. The revolute joint can be actuated by a torque $\tau^{(R)} \in \mathbb{R}$ about $\boldsymbol{n}^1$. It results in the following matrices in (5.8)

$$\boldsymbol{C}^{1,(R)}(\boldsymbol{q}) = \begin{bmatrix} \boldsymbol{0} \\ -\boldsymbol{n}^1 \end{bmatrix} \qquad \boldsymbol{C}^{2,(R)}(\boldsymbol{q}) = \begin{bmatrix} c\boldsymbol{0} \\ \boldsymbol{n}^1 \end{bmatrix}, \tag{5.32}$$

as can be inferred from (5.26) by cancellation of the column corresponding to the translational actuation force. The actuation of the generalised degrees of freedom reads

$$\left(\boldsymbol{P}^{(R)}(\boldsymbol{q})\right)^T \cdot \boldsymbol{f} = \begin{bmatrix} \boldsymbol{\tau}_\varphi \\ \boldsymbol{\varrho}^{rb} \times \boldsymbol{\tau}_\varphi + \boldsymbol{\tau}_\theta - \tau^{(R)}\boldsymbol{n}^1 \\ \tau^{(R)} \end{bmatrix}. \tag{5.33}$$

Proposition 5.5. *This definition of the redundant left and right discrete forces guarantees that the change of angular momentum along the solution trajectory $\boldsymbol{q}_d$ of (3.12) is induced only by the effect of the discrete generalised forces $\boldsymbol{\tau}_{rb}$. In particular, it is conserved exactly, if the motion of the pair is induced by shape changes only.*

Proof. The proof is similar to that for the cylindrical pair; here one uses $\tau^{(C)}_\varphi = 0$ and $\tau^{(C)}_\theta = \tau^{(R)}$. ■

5.4 Prismatic Pair

In the case of the P pair (Figure 5.4), translational motion of the second body relative to the first one may occur along the axis specified by the unit vector $\boldsymbol{n}^1$, which as before is specified by (5.16).

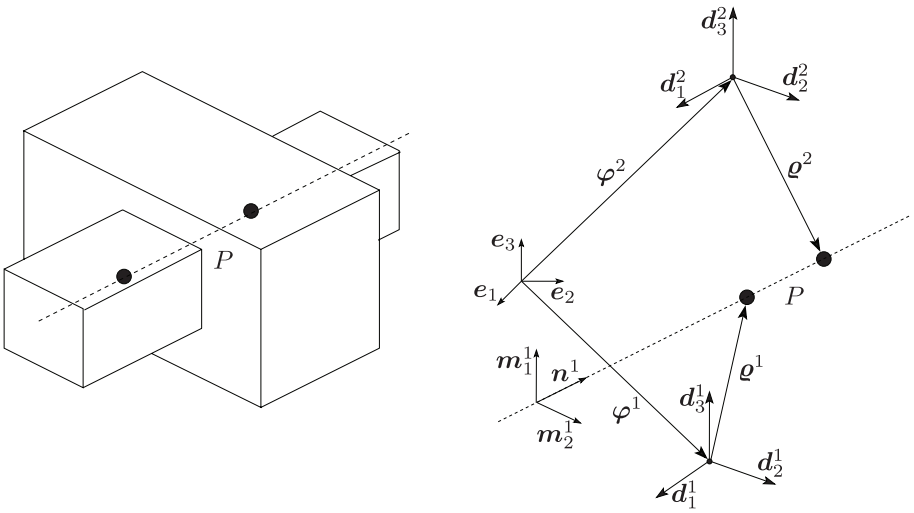

Figure 5.4: Prismatic pair.

Constraints. The P pair entails $m_{\text{ext}}^{(P)} = 5$ external constraint functions that may be written in the form

$$\boldsymbol{g}_{\text{ext}}^{(P)}(\boldsymbol{q}) = \begin{bmatrix} (\boldsymbol{m}_1^1)^T \cdot (\boldsymbol{s}^2 - \boldsymbol{s}^1) \\ (\boldsymbol{m}_2^1)^T \cdot (\boldsymbol{s}^2 - \boldsymbol{s}^1) \\ (\boldsymbol{d}_1^1)^T \cdot \boldsymbol{d}_2^2 - \eta_1 \\ (\boldsymbol{d}_2^1)^T \cdot \boldsymbol{d}_3^2 - \eta_2 \\ (\boldsymbol{d}_3^1)^T \cdot \boldsymbol{d}_1^2 - \eta_3 \end{bmatrix}, \tag{5.34}$$

where η_i, $i = 1, 2, 3$ are constant and need be consistent with the initial conditions. Again, $\boldsymbol{m}_\kappa^1 \in \mathbb{R}^3$ and $\boldsymbol{s}^\alpha \in \mathbb{R}^3$ are given by (5.17) and (5.19), respectively. Furthermore, the kinematic constraint

$$\boldsymbol{\omega}^2 = \boldsymbol{\omega}^1 \tag{5.35}$$

applies to the P pair.

Null Space Matrix. To get proper representations of the null space matrix for the P pair, the previous treatment of the C pair requires the removal of $\dot{\theta}^2$ and only $\dot{u}^2$ remains.

$$\boldsymbol{P}_{\text{int}}(\boldsymbol{q}^2) \cdot \mathbf{P}_{\text{ext}}^{2,(P)}(\boldsymbol{q}) = \begin{bmatrix} \boldsymbol{I} - \boldsymbol{n}^1 \otimes \boldsymbol{n}^1 & \widehat{\boldsymbol{\varphi}^1 - \boldsymbol{\varphi}^2} & \boldsymbol{n}^1 \\ \mathbf{0} & -(\widehat{\boldsymbol{d}_1^2}) & \mathbf{0} \\ \mathbf{0} & -(\widehat{\boldsymbol{d}_2^2}) & \mathbf{0} \\ \mathbf{0} & -(\widehat{\boldsymbol{d}_3^2}) & \mathbf{0} \end{bmatrix} \tag{5.36}$$

Nodal Reparametrisation. The mapping $\boldsymbol{F}^{2,(P)}(\boldsymbol{\mu}^{(P)}_{n+1}, \boldsymbol{q}_n)$ can be inferred from the corresponding one for the C pair (5.25), by setting $\theta^2_{n+1} = 0$. Accordingly,

$$\boldsymbol{q}^2_{n+1} = \boldsymbol{F}^{2,(P)}(\boldsymbol{\mu}^{(P)}_{n+1}, \boldsymbol{q}_n) = \begin{bmatrix} \boldsymbol{\varphi}^1_n + (\boldsymbol{I} - \boldsymbol{n}^1_n \otimes \boldsymbol{n}^1_n) \cdot \boldsymbol{u}^1_{\varphi_{n+1}} + \exp(\widehat{\boldsymbol{\theta}^1_{n+1}}) \cdot [\boldsymbol{\varrho}^1_n - \boldsymbol{\varrho}^2_n + (\bar{u}^2_n + u^2_{n+1})\boldsymbol{n}^1_n] \\ \exp(\widehat{\boldsymbol{\theta}^1_{n+1}}) \cdot (\boldsymbol{d}^2_1)_n \\ \exp(\widehat{\boldsymbol{\theta}^1_{n+1}}) \cdot (\boldsymbol{d}^2_2)_n \\ \exp(\widehat{\boldsymbol{\theta}^1_{n+1}}) \cdot (\boldsymbol{d}^2_3)_n \end{bmatrix}, \tag{5.37}$$

with incremental unknowns $\boldsymbol{\mu}^{(P)}_{n+1} = (\boldsymbol{u}^1_{\varphi_{n+1}}, \boldsymbol{\theta}^1_{n+1}, u^2_{n+1}) \in \mathbb{R}^3 \times \mathbb{R}^3 \times \mathbb{R}$ and $\bar{u}^2_n = \boldsymbol{n}^1_n \cdot (\boldsymbol{s}^2_n - \boldsymbol{s}^1_n)$ denoting the translation of the second body relative to the first one in the direction of the axis $\boldsymbol{n}^1_n$ at time t_n.

Actuation of the Prismatic Pair. The translational force $\tau^{(P)} \in \mathbb{R}$ acts in the direction of the axis $\boldsymbol{n}^1$. Its contribution to the bodies forces is given by (5.8) with

$$\boldsymbol{C}^{1,(P)}(\boldsymbol{q}) = \begin{bmatrix} -\boldsymbol{n}^1 \\ (\boldsymbol{\varphi}^1 - \boldsymbol{\varphi}^2) \times \boldsymbol{n}^1 \end{bmatrix} \qquad \boldsymbol{C}^{2,(P)}(\boldsymbol{q}) = \begin{bmatrix} \boldsymbol{n}^1 \\ \boldsymbol{0} \end{bmatrix}, \tag{5.38}$$

as can be inferred from (5.26) by cancellation of the column corresponding to the torque actuation. As in (5.27), the torque induced by a translational joint force away from the centre of mass does not show up in the resulting actuation of the generalised degrees of freedom

$$\left(\boldsymbol{P}^{(P)}(\boldsymbol{q})\right)^T \cdot \boldsymbol{f} = \begin{bmatrix} \boldsymbol{\tau}_\varphi - \tau^{(P)}\boldsymbol{n}^1 \\ \boldsymbol{\varrho}^{rb} \times \boldsymbol{\tau}_\varphi + \boldsymbol{\tau}_\theta \\ \tau^{(P)} \end{bmatrix}. \tag{5.39}$$

Proposition 5.6. *This definition of the redundant left and right discrete forces guarantees that the change of angular momentum along the solution trajectory $\boldsymbol{q}_d$ of (3.12) is induced only by the effect of the discrete generalised forces $\boldsymbol{\tau}_{rb}$. In particular, it is conserved exactly, if the motion of the pair is induced by shape changes only.*

```
Jerry:  I suggest omitting the phrase ‘‘(geometric
phase)’’.
```

ToDo

Proof. The proof can be inferred from the that for the cylindrical pair by setting $\tau^{(C)}_\varphi = \tau^{(P)}$ and $\tau^{(C)}_\theta = 0$. ■

5.5 Planar Pair

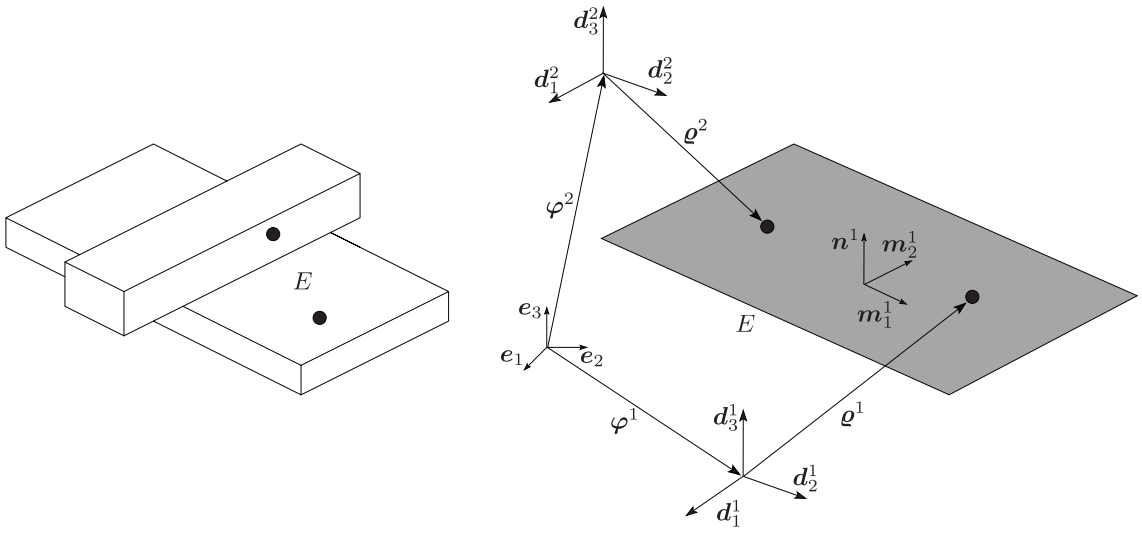

Figure 5.5: Planar pair.

As before in the context of the cylindrical pair, for the E pair (Figure 5.5) use is made of the orthonormal frame $\{\boldsymbol{m}_1^1, \boldsymbol{m}_2^1, \boldsymbol{n}^1\}$, with $\boldsymbol{n}^1 = n_I^1 \boldsymbol{d}_I^1$ and $\boldsymbol{m}_\kappa^1 = (m_\kappa^1)_I \boldsymbol{d}_I^1$. In the present case, the motion of the second body in the plane spanned by $\boldsymbol{m}_1^1, \boldsymbol{m}_2^1$ can be characterised by $r^{(E)} = 3$ degrees of freedom. Specifically, the second body may rotate about the axis specified by $\boldsymbol{n}^1$ and translate in the plane spanned by $\boldsymbol{m}_1^1$ and $\boldsymbol{m}_2^1$. The relative translational motion may be accounted for by two coordinates $(u_1^2, u_2^2) \in \mathbb{R}^2$, such that

$$\boldsymbol{s}^2 = \boldsymbol{s}^1 + u_\kappa^2 \boldsymbol{m}_\kappa^1. \tag{5.40}$$

As before, $\boldsymbol{s}^\alpha = \boldsymbol{\varphi}^\alpha + \boldsymbol{\varrho}^\alpha$ for $\alpha = 1, 2$.

Constraints. The E pair gives rise to $m_{\text{ext}}^{(E)} = 3$ external constraint functions that may be written in the form

$$\boldsymbol{g}_{\text{ext}}^{(E)}(\boldsymbol{q}) = \begin{bmatrix} (\boldsymbol{n}^1)^T \cdot (\boldsymbol{s}^2 - \boldsymbol{s}^1) \\ (\boldsymbol{n}^1)^T \cdot \boldsymbol{d}_1^2 - \eta_1 \\ (\boldsymbol{n}^1)^T \cdot \boldsymbol{d}_2^2 - \eta_2 \end{bmatrix}, \tag{5.41}$$

where η_1, η_2 are constant and need be consistent with the initial conditions.

Null Space Matrix. Differentiating (5.40) with respect to time and taking into account (5.43) and Remark 5.3 yields

$$\dot{\boldsymbol{\varphi}}^2 = \boldsymbol{I}^{12} \cdot \dot{\boldsymbol{\varphi}}^1 + \boldsymbol{\omega}^1 \times (\boldsymbol{\varrho}^1 + u_\kappa^2 \boldsymbol{m}_\kappa^1) - \left[\boldsymbol{I}^{11} \cdot \boldsymbol{\omega}^1\right] \times \boldsymbol{\varrho}^2 + \dot{u}_\kappa^2 \boldsymbol{m}_\kappa^1 + \dot{\theta}^2 \boldsymbol{\varrho}^2 \times \boldsymbol{n}^1, \tag{5.42}$$

with $\boldsymbol{I}^{12} = \boldsymbol{I} - \boldsymbol{m}_1^1 \otimes \boldsymbol{m}_1^1 - \boldsymbol{m}_2^1 \otimes \boldsymbol{m}_2^1$ and

$$\boldsymbol{\omega}^2 = \boldsymbol{I}^{11} \cdot \boldsymbol{\omega}^1 + \dot{\theta}^2 \boldsymbol{n}^1. \tag{5.43}$$

With regard to (5.3), the null space matrix for the E pair is given by

$$\boldsymbol{P}_{\text{int}}(\boldsymbol{q}^2) \cdot \boldsymbol{P}_{\text{ext}}^{2,(E)}(\boldsymbol{q}) = \begin{bmatrix} \boldsymbol{I}^{12} & \widehat{\boldsymbol{\varrho}^2} \cdot \boldsymbol{I}^{11} - \widehat{\boldsymbol{\varrho}^1} - \widehat{u_\kappa^2 \boldsymbol{m}_\kappa^1} & \boldsymbol{m}_1^1 & \boldsymbol{m}_2^1 & \boldsymbol{\varrho}^2 \times \boldsymbol{n}^1 \\ \boldsymbol{0} & -\widehat{\boldsymbol{d}_1^2} \cdot \boldsymbol{I}^{11} & \boldsymbol{0} & \boldsymbol{0} & \boldsymbol{n}^1 \times \boldsymbol{d}_1^2 \\ \boldsymbol{0} & -\widehat{\boldsymbol{d}_2^2} \cdot \boldsymbol{I}^{11} & \boldsymbol{0} & \boldsymbol{0} & \boldsymbol{n}^1 \times \boldsymbol{d}_2^2 \\ \boldsymbol{0} & -\widehat{\boldsymbol{d}_3^2} \cdot \boldsymbol{I}^{11} & \boldsymbol{0} & \boldsymbol{0} & \boldsymbol{n}^1 \times \boldsymbol{d}_3^2 \end{bmatrix}. \tag{5.44}$$

Jerry: Consider introducing shorthand notation such as $M_\kappa = \boldsymbol{I} - \boldsymbol{m}_\kappa^1 \otimes \boldsymbol{m}_\kappa^1$ to make these expressions (5.42) and (5.44) more compact. Something like this is needed for (5.45) below, which is too wide.

ToDo

Nodal Reparametrisation. In the present case the configuration of the second body can be characterised by the incremental variables $\boldsymbol{\vartheta}_{n+1}^{(E)} = (u_{1_{n+1}}^2, u_{2_{n+1}}^2, \theta_{n+1}^2) \in \mathbb{R}^3$. Accordingly, the mapping $\boldsymbol{F}_{q_n}^{2,(E)}(\boldsymbol{\mu}_{n+1}^{(E)})$ can be written in the form

$$\boldsymbol{q}_{n+1}^2 = \boldsymbol{F}_{q_n}^{2,(E)}(\boldsymbol{\mu}_{n+1}^{(E)}) = \begin{bmatrix} \boldsymbol{\varphi}_n^1 + (\boldsymbol{I}^{12})_n \cdot \boldsymbol{u}_{\varphi_{n+1}}^1 + \boldsymbol{R}^{1,2} \cdot [\boldsymbol{\varrho}_n^1 + ((\bar{u}_\kappa^2)_n + u_{\kappa_{n+1}}^2)(\boldsymbol{m}_\kappa^1)_n] - \boldsymbol{R}^{1,2} \cdot \exp\left(\theta_{n+1}^2 \widehat{\boldsymbol{n}_n^1}\right) \cdot \boldsymbol{\varrho}_n^2 \\ \boldsymbol{R}^{1,2} \cdot \exp\left(\theta_{n+1}^2 \widehat{\boldsymbol{n}_n^1}\right) \cdot (\boldsymbol{d}_1^2)_n \\ \boldsymbol{R}^{1,2} \cdot \exp\left(\theta_{n+1}^2 \widehat{\boldsymbol{n}_n^1}\right) \cdot (\boldsymbol{d}_2^2)_n \\ \boldsymbol{R}^{1,2} \cdot \exp\left(\theta_{n+1}^2 \widehat{\boldsymbol{n}_n^1}\right) \cdot (\boldsymbol{d}_3^2)_n \end{bmatrix}. \tag{5.45}$$

Here, $(\bar{u}_\kappa^2)_n = (\boldsymbol{m}_\kappa^1)_n \cdot (\boldsymbol{s}_n^2 - \boldsymbol{s}_n^1)$ denotes the translation of the second body relative to the first one in the direction of the axis $(\boldsymbol{m}_\kappa^1)_n$ at time t_n.

Actuation of the Planar Pair. The three relative degrees of freedom allowed by the planar joint can be actuated by a translational forces $\tau_{\varphi_1}^{(E)}, \tau_{\varphi_2}^{(E)} \in \mathbb{R}$ that acts in the directions of $\boldsymbol{m}_1^1, \boldsymbol{m}_2^1$ and a torque $\tau_\theta^{(E)} \in \mathbb{R}$ about $\boldsymbol{n}^1$. In (5.8), they are accounted for using

$$\begin{aligned} \boldsymbol{C}^{1,(E)}(\boldsymbol{q}) &= \begin{bmatrix} -\boldsymbol{m}_1^1 & -\boldsymbol{m}_2^1 & \boldsymbol{0} \\ (\boldsymbol{\varphi}_1 - \boldsymbol{\varphi}_2) \times \boldsymbol{m}^1 & (\boldsymbol{\varphi}_1 - \boldsymbol{\varphi}_2) \times \boldsymbol{m}^2 & -\boldsymbol{n}^1 \end{bmatrix} \\ \boldsymbol{C}^{2,(E)}(\boldsymbol{q}) &= \begin{bmatrix} \boldsymbol{m}_1^1 & \boldsymbol{m}_2^1 & \boldsymbol{0} \\ \boldsymbol{0} & \boldsymbol{0} & \boldsymbol{n}^1 \end{bmatrix}. \end{aligned} \tag{5.46}$$

Jerry: Preceding and following displays are too wide ToDo

Similar to (5.27), the torque induced by a translational joint force away from the centre of mass effects the generalised rotational degrees of freedom only with respect to the allowed rotation around $\boldsymbol{n}^1$

$$\left(\boldsymbol{P}^{(E)}(\boldsymbol{q})\right)^T \cdot \boldsymbol{f} = \begin{bmatrix} \boldsymbol{\tau}_\varphi - \tau_{\varphi_1}^{(E)}\boldsymbol{m}_1^1 - \tau_{\varphi_2}^{(E)}\boldsymbol{m}_2^1 \\ \boldsymbol{\varrho}^{rb} \times \boldsymbol{\tau}_\varphi + \boldsymbol{\tau}_\theta + (\boldsymbol{n}^1)^T \cdot \left(\boldsymbol{\varrho}^2 \times \left(\tau_{\varphi_1}^{(E)}\boldsymbol{m}_1^1 + \boldsymbol{\tau}_{\varphi_2}^{(E)}\boldsymbol{m}_2^1\right)\right) \cdot \boldsymbol{n}^1 - \tau_\theta^{(E)}\boldsymbol{n}^1 \\ \tau_{\varphi_1}^{(E)} \\ \tau_{\varphi_2}^{(E)} \\ -(\boldsymbol{n}^1)^T \cdot \left(\boldsymbol{\varrho}^2 \times \left(\tau_{\varphi_1}^{(E)}\boldsymbol{m}_1^1 + \boldsymbol{\tau}_{\varphi_2}^{(E)}\boldsymbol{m}_2^1\right)\right) + \tau_\theta^{(E)} \end{bmatrix}. \tag{5.47}$$

Proposition 5.7. *This definition of the redundant left and right discrete forces guarantees that the change of angular momentum along the solution trajectory $\boldsymbol{q}_d$ of (3.12) is induced only by the effect of the discrete generalised forces $\boldsymbol{\tau}_{rb}$. In particular, it is conserved exactly, if the motion of the pair is induced by shape changes only.*

Proof. Computation of $\boldsymbol{p}_{n+1}^+$ and via $\boldsymbol{p}_n^-$ the discrete Legendre transforms (3.13) and insertion into the definition of angular momentum (4.4) yields

$$\begin{aligned} \boldsymbol{L}_{n+1} - \boldsymbol{L}_n &= \boldsymbol{\varphi}_{n+1}^1 \times \boldsymbol{p}_{\varphi_{n+1}}^{1\,+} + \boldsymbol{d}_{I\,n+1}^1 \times \boldsymbol{p}_{I\,n+1}^{1+} + \boldsymbol{\varphi}_{n+1}^2 \times \boldsymbol{p}_{\varphi_{n+1}}^{2\,+} + \boldsymbol{d}_{I\,n+1}^2 \times \boldsymbol{p}_{I\,n+1}^{2+} + \\ &\quad - \boldsymbol{\varphi}_n^1 \times \boldsymbol{p}_{\varphi_n}^{1\,-} - \boldsymbol{d}_{I\,n}^1 \times \boldsymbol{p}_{I\,n}^{1-} - \boldsymbol{\varphi}_n^2 \times \boldsymbol{p}_{\varphi_n}^{2\,-} - \boldsymbol{d}_{I\,n}^2 \times \boldsymbol{p}_{I\,n}^{2-} \qquad (5.48) \\ &= \frac{h}{2}\left(\tau_{\varphi_{1_n}}^{(E)}\boldsymbol{m}_{1\,n+1}^1 + \tau_{\varphi_{2_n}}^{(E)}\boldsymbol{m}_{2\,n+1}^1\right) \times \left(\boldsymbol{\varphi}_{n+1}^1 - \boldsymbol{\varphi}_{n+1}^2 + \boldsymbol{\varphi}_{n+1}^2 - \boldsymbol{\varphi}_{n+1}^1\right) + \\ &\quad \frac{h}{2}\left(\tau_{\varphi_{1_n}}^{(E)}\boldsymbol{m}_{1\,n}^1 + \tau_{\varphi_{2_n}}^{(E)}\boldsymbol{m}_{2\,n}^1\right) \times \left(\boldsymbol{\varphi}_n^1 - \boldsymbol{\varphi}_n^2 + \boldsymbol{\varphi}_n^2 - \boldsymbol{\varphi}_n^1\right) + \\ &\quad \frac{h}{2}\left(-\tau_{\theta_n}^{(E)}\boldsymbol{n}_{n+1}^1 + \tau_{\theta_n}^{(E)}\boldsymbol{n}_{n+1}^1 - \tau_{\theta_n}^{(E)}\boldsymbol{n}_n^1 + \tau_{\theta_n}^{(E)}\boldsymbol{n}_n^1\right) = \boldsymbol{0}. \end{aligned}$$

■

Jerry: Consider resetting equation like (4.14). ToDo

6 Optimal Control for Multibody Systems

In a kinematic chain or tree structured system, where N bodies are interconnected by $N-1$ joints, the multibody system consists of $N-1$ pairs. The configuration variable

$$\boldsymbol{q} = \begin{bmatrix} \boldsymbol{q}^1 \\ \vdots \\ \boldsymbol{q}^N \end{bmatrix} \in \mathbb{R}^{12N} \tag{6.1}$$

is a generalisation of (5.1) and the corresponding $12N \times 12N$ mass matrix consists of block matrices of the form (4.3). The constraints, null space matrices and nodal reparametrisation for the multibody system can be inferred from the corresponding expressions for kinematic pairs given in the preceding section.

Jerry: Refer to the preceding section instead?	ToDo

Actuation of a Multibody System. As a generalisation of (5.7), the forces and torques acting on the multibody system can be collected in

$$\begin{bmatrix} \boldsymbol{\tau}_{rb} \\ \boldsymbol{\tau}^{(J_1)} \\ \vdots \\ \boldsymbol{\tau}^{(J_{N-1})} \end{bmatrix} \in \mathbb{R}^{6+\sum_{i=1}^{N-1} r^{(J_i)}}. \tag{6.2}$$

The redundant forces for each body can be computed as

$$\boldsymbol{f} = \begin{bmatrix} \boldsymbol{f}^1 \\ \vdots \\ \boldsymbol{f}^N \end{bmatrix} = \boldsymbol{B}^T(\boldsymbol{q}) \cdot \begin{bmatrix} \boldsymbol{\tau}_{rb} \\ \boldsymbol{\tau}^{(J_1)} \\ \vdots \\ \boldsymbol{\tau}^{(J_{N-1})} \end{bmatrix} \in \mathbb{R}^{12N}, \tag{6.3}$$

with the $12N \times (6+\sum_{i=1}^{N-1} r^{(J_i)})$ matrix $\boldsymbol{B}^T(\boldsymbol{q})$ being the product of three matrices as in (5.9). The first matrix corresponds to the internal constraints of each body and consists of N blocks $\boldsymbol{P}_{\text{int}}(\boldsymbol{q}^\alpha), \alpha = 1, \ldots, N$. The second $6N \times 6N$ diagonal matrix is an obvious extension of the one given in (5.9) consisting of multiples of the identity matrix. The third matrix is given by concatenating the matrices $\boldsymbol{C}_{rb}(\boldsymbol{q}^1)$ and $\bar{\boldsymbol{C}}^{(J_i)}$ for each joint $J_i, i = 1, \ldots, N-1$ into a $6N \times (6 + \sum_{i=1}^{N-1} r^{(J_i)})$ matrix. The first $6N \times 6$ block consists of $\boldsymbol{C}_{rb}(\boldsymbol{q}^1)$ and a zero matrix below. Corresponding to the joint J_i, the $6N \times r^{(J_i)}$ block $\bar{\boldsymbol{C}}^{(J_i)}$ has

two nonzero subblocks. Let the α-th and β-th body be connected by the joint J_i, then $\boldsymbol{C}^{1,(J_i)}(\boldsymbol{q})$ and $\boldsymbol{C}^{2,(J_i)}(\boldsymbol{q})$ occur in the rows corresponding to the forces $\boldsymbol{f}^\alpha$ and $\boldsymbol{f}^\beta$ acting on the α-th and β-th body, respectively.

$$\left[\begin{array}{c|c|c|c} \boldsymbol{C}_{rb}(\boldsymbol{q}^1) & \bar{\boldsymbol{C}}^{(J_1)} & \dots & \bar{\boldsymbol{C}}^{(J_{N-1})} \\ \boldsymbol{0}_{6(N-1)\times 6} & & & \end{array}\right] \tag{6.4}$$

See §7.2 and §7.3 for examples of this matrix in the context of a tree structured multibody system and a kinematic chain.

7 Numerical examples

7.1 Optimal Control of a Rigid Sphere

As a first example demonstrating the performance of the proposed procedure, the actuation of a rigid sphere in three-dimensional space is investigated.

Set Up and Problem Statement. The sphere has radius $r = 0.05$ and density of $\rho = 27000$. In the initial position, its centre of mass is located at $\boldsymbol{u}_\varphi^0 = [R, 0, 0]^T$ with $R = 1$ and the directors are aligned with the axes of the inertial frame, thus $\boldsymbol{\theta}^0 = [0, 0, 0]^T$. The body is forced to move to the position $\boldsymbol{\varphi}^N = [0, R, 2R]^T$ while performing three full rotations around the axis $[-1, 1, 1]^T/\sqrt{3}$. Since the relative reparametrisation (3.9) is used, $\boldsymbol{u}^N$ represents the rotation of the body in $[t_{N-1}, t_N]$ and can not be used to uniquely define the final configuration. The final orientation of the rigid body is specified by prescribing that the directors are aligned with the axes of the inertial frame at t_N, i.e. $\boldsymbol{d}_I^N = \boldsymbol{e}_I$, what can be transformed into three scalar conditions. In this case, the function $\boldsymbol{D}$ describing the final configuration condition in $(3.26)_2$ reads

$$\boldsymbol{D}(\boldsymbol{q}_N, \boldsymbol{q}^N) = \begin{bmatrix} \boldsymbol{I}_{3\times 3} & \boldsymbol{0}_{3\times 3} & \boldsymbol{0} & \boldsymbol{0} \\ \boldsymbol{0}_{1\times 3} & \boldsymbol{e}_1^T & \boldsymbol{0} & \boldsymbol{0} \\ \boldsymbol{0}_{1\times 3} & \boldsymbol{0} & \boldsymbol{e}_2^T & \boldsymbol{0} \\ \boldsymbol{0}_{1\times 3} & \boldsymbol{0} & \boldsymbol{0} & \boldsymbol{e}_3^T \end{bmatrix} \cdot (\boldsymbol{q}_N - \boldsymbol{q}^N). \tag{7.1}$$

The motion starts and ends at rest and takes places within $N = 30$ time-steps of size $h = 0.1$. The objective function in use is of type (3.25) and represents the control effort, it reads $\bar{J}_d = h \sum_{n=0}^{N-1} ||\boldsymbol{\tau}_n||^2$. For the documented motion, it takes the value $\bar{J}_d = 533.5767$.

Figure 7.1 shows the initial (blue) and final (red) configuration of the sphere as well as the specified axis of rotation (dashed line).

Optimal Motion of the Sphere. While the sphere moves in space, this axis is translated parallel to itself. The motion of the sphere is depicted in Figure 7.2 at every third time-step. The corresponding motion of the centre of mass and evolution of the directors are depicted in Figure 7.3. The evolution of the generalised forces, consisting of the translational forces and the torques can be observed in Figure 7.4. According to the assumptions made, the generalised forces are constant in each time interval. Figure 7.5 shows the evolution of the kinetic energy and the components of the angular momentum. Apparently the initial and final conditions of zero motion are met. The first diagram in Figure 7.6 depicts the change of angular momentum in each time interval while the second diagram reveals its consistency in the sense that as shown in Proposition 4.1, the change of angular momentum equals exactly the sum of the applied torques and the momentum induced by the translational forces during that time interval. The minimisation of (3.25) subject to the constraints (3.26) has been performed by the SQP solver *fmincon* in Matlab. For the discrete Lagrangian, the midpoint approximation in (3.2) has been used and the null space matrix (4.5), nodal reparametrisation (4.6) and input transformation matrix (4.11) of the rigid sphere can be inferred from §4.

```
Jerry:  Say some more about how this was implemented.  Eg,
was it done in Matlab, C++?, what discrete Lagrangian was
used, what specific reparametrization was used, etc?  --- ok
to refer to previous expressions, but the reader who starts
with an example (as many will do) needs some guidance.
```

ToDo

Remark 7.1 (Dimension of the constrained optimisation problem)**.** Using our method, the problem consists of 360 unknowns and 192 constraints. In contrast to that, the Lagrange multiplier formulation yields 900 variables and 576 constraints.

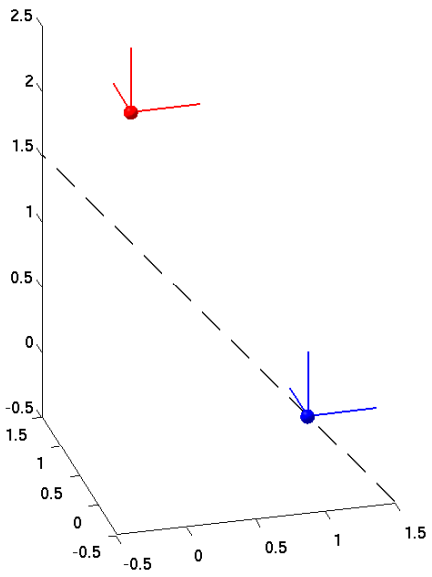

Figure 7.1: Rigid sphere: initial and final configuration and axis of rotation.

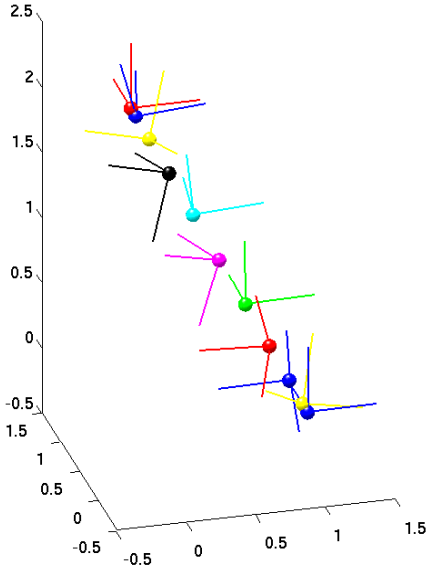

Figure 7.2: Rigid sphere: configuration at $t = 3nh, n = 0, \ldots, 10$ $(h = 0.1)$.

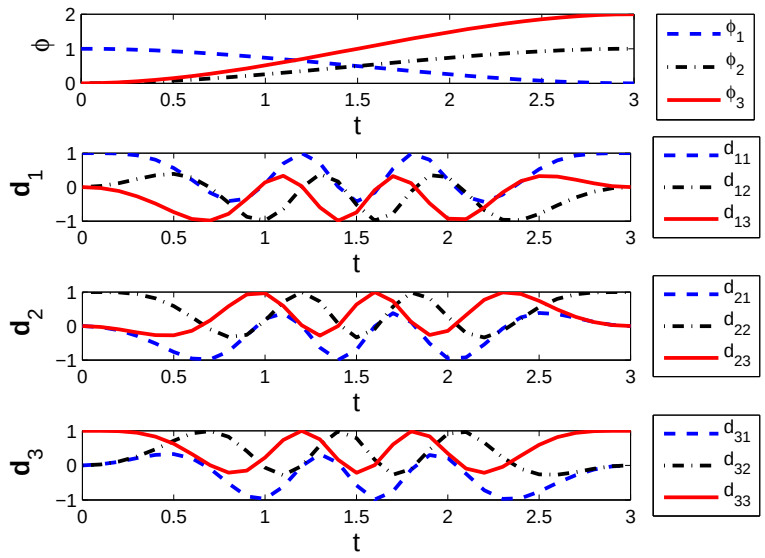

Figure 7.3: Rigid sphere: motion of centre of mass and directors ($h = 0.1$).

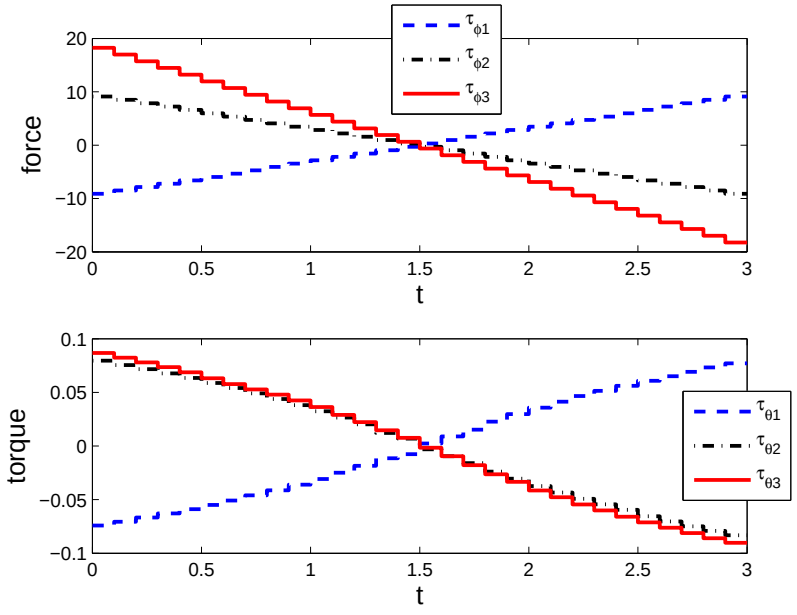

Figure 7.4: Rigid sphere: force and torque ($h = 0.1$).

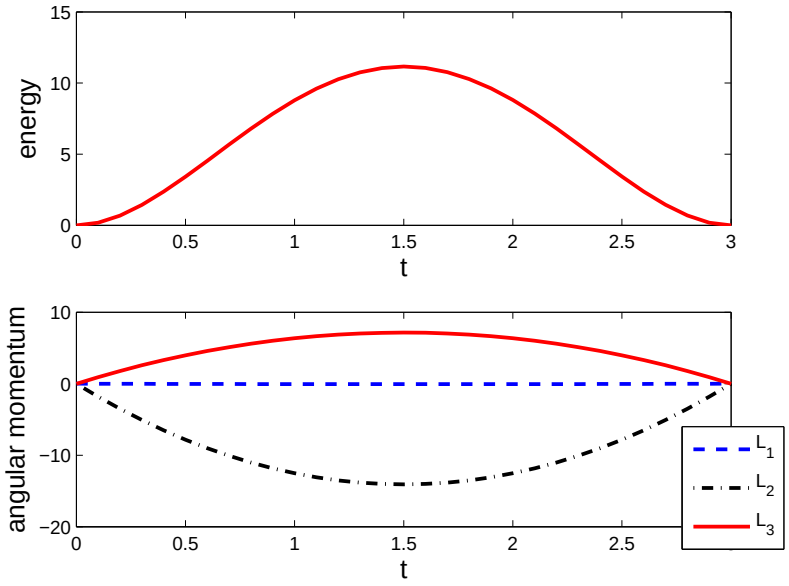

Figure 7.5: Rigid sphere: energy and components of angular momentum vector $\boldsymbol{L} = L_I \boldsymbol{e}_I$ ($h = 0.1$).

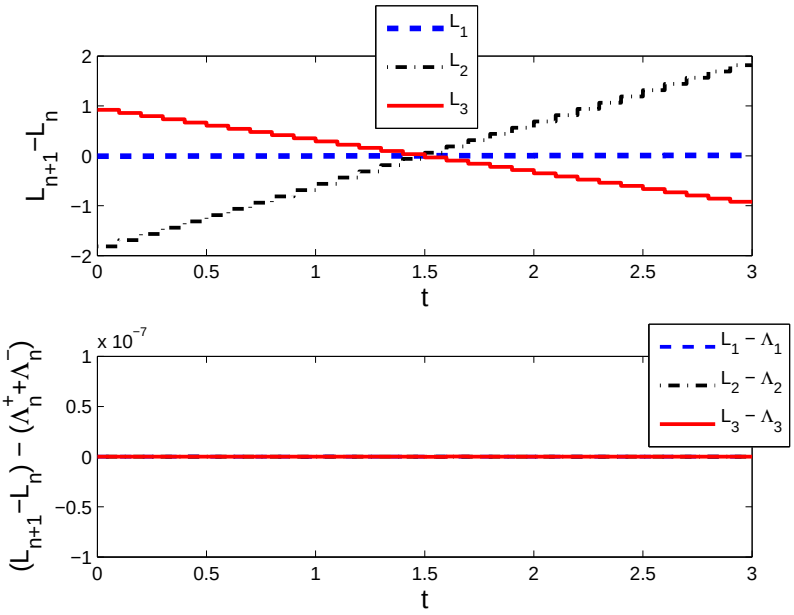

Figure 7.6: Rigid sphere: change and consistency of angular momentum with Λ_n^+, Λ_n^- being the right hand side of (4.14) ($h = 0.1$).

7.2 Optimal Control of a Rigid Body with Rotors

For both, the fully actuated and the underactuated case, the minimisation of (3.25) subject to the constraints (3.26) has been performed by the *nag_opt_nlp_sparse* function which is part of the NAG C library. The discrete midpoint Lagrangian given in (3.2) has been used and the null space matrix, nodal reparametrisation and input transformation matrix can be inferred from §5.3 and §6.

Fully Actuated Case—Set Up and Problem Statement. Inspired by space telescopes such as the Hubble telescope, whose change in orientation is induced by spinning rotors, a multibody system consisting of a main body to which rotors are connected by revolute joints has been analysed. The revolute joints allow each rotor to rotate relative to the main body around an axis through its center which is fixed in the main body and are actuated by torques $\tau^{(R_1)}, \tau^{(R_2)}, \tau^{(R_3)} \in \mathbb{R}$. No other force and torque is applied to this tree-structured system, therefore in (6.4), the matrix reduces to

$$\begin{bmatrix} \boldsymbol{C}^{1,(R_1)}(\boldsymbol{q}) & \boldsymbol{C}^{1,(R_2)}(\boldsymbol{q}) & \boldsymbol{C}^{1,(R_3)}(\boldsymbol{q}) \\ \boldsymbol{C}^{2,(R_1)}(\boldsymbol{q}) & \boldsymbol{0} & \boldsymbol{0} \\ \boldsymbol{0} & \boldsymbol{C}^{2,(R_2)}(\boldsymbol{q}) & \boldsymbol{0} \\ \boldsymbol{0} & \boldsymbol{0} & \boldsymbol{C}^{2,(R_3)}(\boldsymbol{q}) \end{bmatrix}, \tag{7.2}$$

which is then used in (6.3) to compute the redundant forces on each body.

The goal is to determine optimal torques to guide the main body from the initial orientation $\boldsymbol{u}_\theta^0 = [0, 0, 0]$ into the final position $\boldsymbol{u}_\theta^N = \frac{\pi}{14}[1, 2, 3]$, where the absolute reparametrisation $\boldsymbol{q}_n = \boldsymbol{F}(\boldsymbol{u}_n, \boldsymbol{q}_{00})$ is used instead of (3.9) here. The motion starts and ends at rest. The manoeuvre time is $T = 5$ and the time-step is $h = 0.1$, thus $N = 50$. As in the first example, the objective function represents the control effort which has to be minimised. Due to the presence of three rotors with non-planar axes of rotation, this problem is fully actuated.

Fully Actuated Case—Problem Solution. Figure 7.7 shows the configuration of the system at $t = 0, 1, \ldots, 5$. The static frame represents the required final orientation where the axes must coincide with the centres of the rotors as the motion ends (see last picture). The optimal torques which are constant in each time interval are depicted in Figure 7.8. They yield a control effort of $\bar{J}_d = 2.8242 \cdot 10^6$. Finally, Figure 7.9 illustrates the evolution of the kinetic energy and a special attribute of the system under consideration. Due to a geometric phase, the motion occurs although the total angular momentum remains zero at all times. As shown in Proposition 5.5, the algorithm is able to represent this correctly.

Remark 7.2 (Dimension of the constrained optimisation problem)**.** Using the advocated method, the problem consists of 900 unknowns and 468 constraints, rather than 6750 variables and 4524 constraints using the Lagrange multiplier formulation.

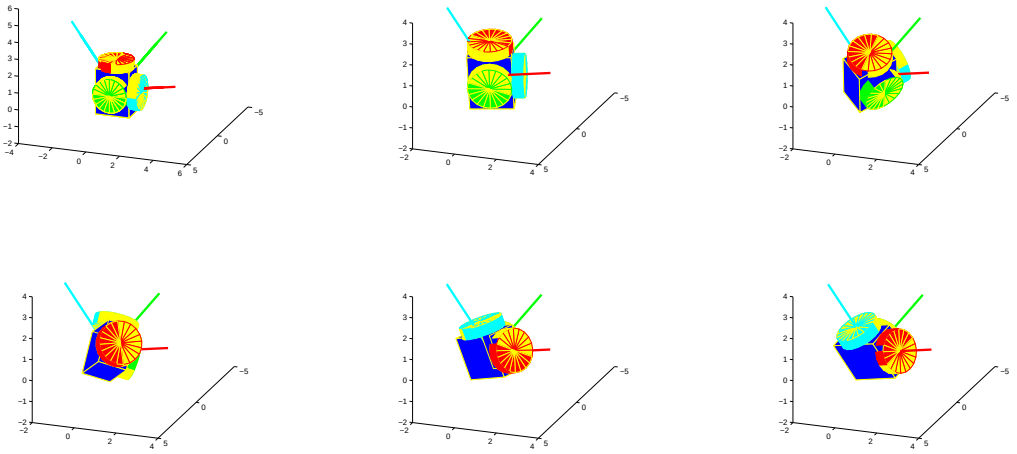

Figure 7.7: Rigid body with three rotors: configuration at $t = 10nh, n = 0, \ldots, 5$ $(h = 0.1)$.

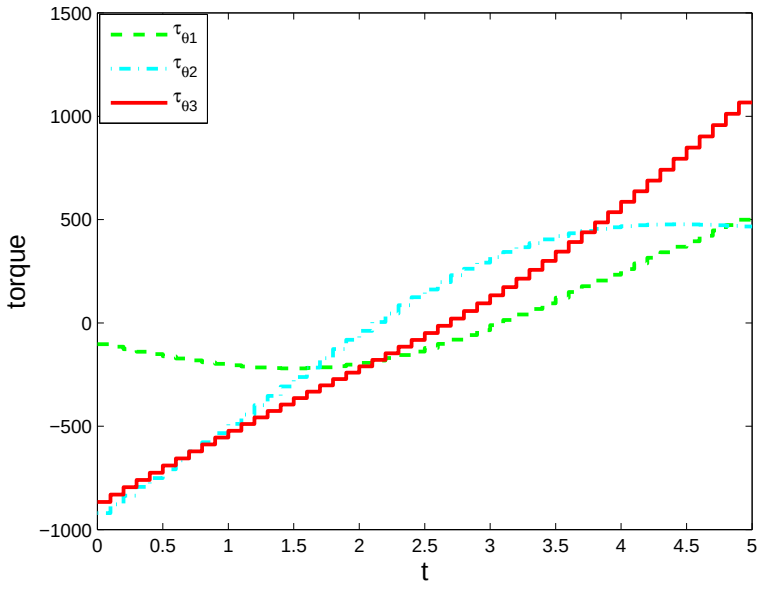

Figure 7.8: Rigid body with three rotors: torque ($h = 0.1$).

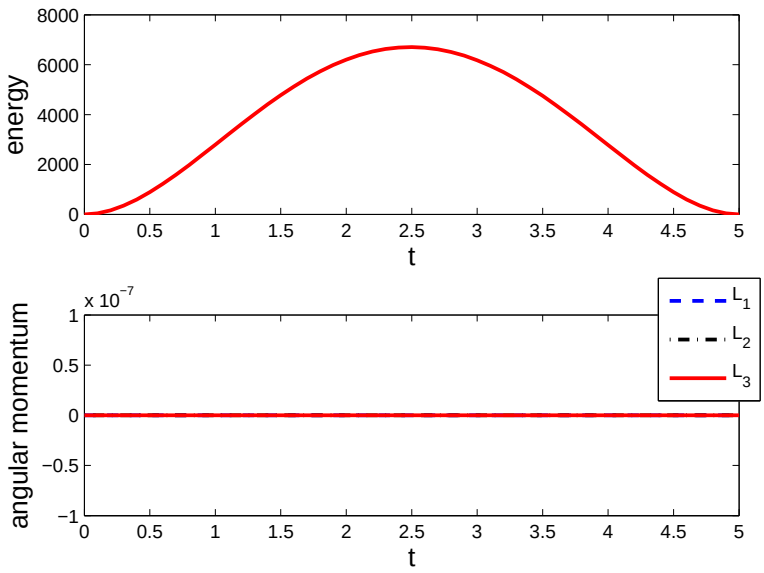

Figure 7.9: Rigid body with three rotors: energy and components of angular momentum vector $\boldsymbol{L} = L_I \boldsymbol{e}_I$ ($h = 0.1$).

Underactuated Case. The same rest to rest manoeuvre is investigated for the underactuated system where one momentum wheel has been removed. Using the same time step and the same number of time steps as for the fully actuated case, the reorientation manoeuvre depicted in Figure 7.10 requires only slightly more control effort $\bar{J}_d = 2.9168 \cdot 10^6$.
Consistency of angular momentum is observable from Figure 7.11. It also shows that the energy does not evolve as symmetrically as for the fully actuated problem. That means that acceleration phase and breaking phase are not exactly inverse to each other. This becomes also obvious from Figure 7.12 showing the evolution of the optimal generalised forces.

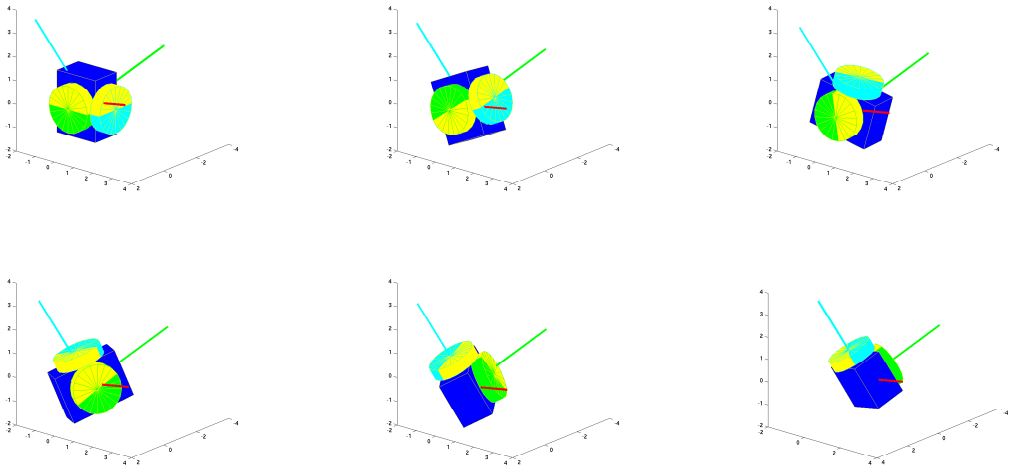

Figure 7.10: Rigid body with two rotors: configuration at $t = 10nh, n = 0, \ldots, 5$ $(h = 0.1)$.

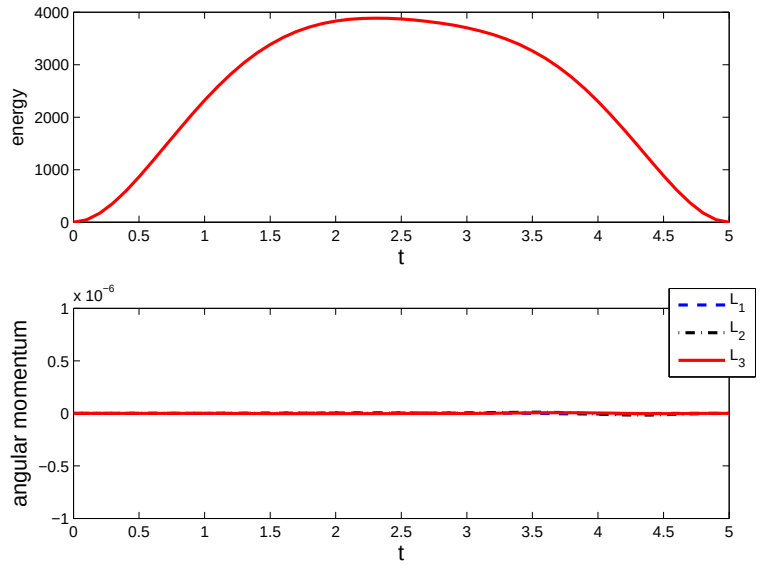

Figure 7.11: Rigid body with two rotors: energy and components of angular momentum vector $\boldsymbol{L} = L_I \boldsymbol{e}_I$ ($h = 0.1$).

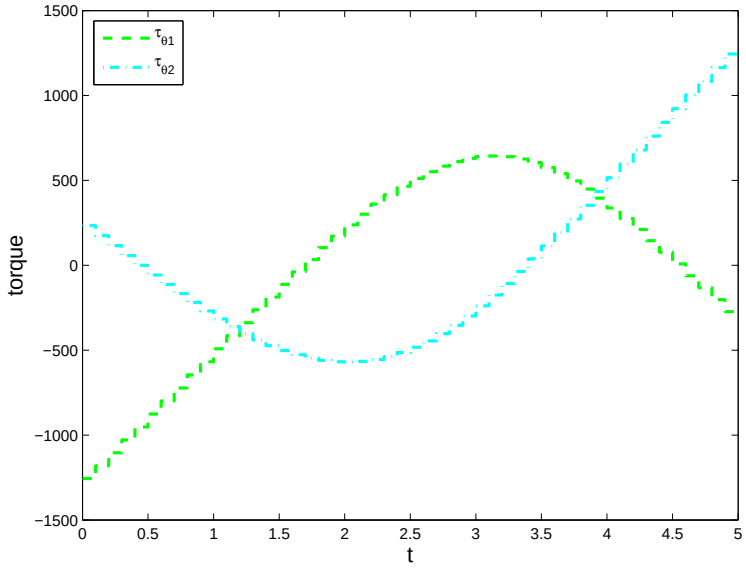

Figure 7.12: Rigid body with two rotors: torque ($h = 0.1$).

7.3 Optimal Control of a Pitcher's Motion

As an example of biomotion in sports, the optimal pitch of an athlete is investigated in this section. For simplicity, a kinematic chain representing the pitcher's arm is considered including the collarbone, the upper and the forearm (see Figure 7.13), where the single bodies are interconnected by joints and actuated via control torques in the joints representing the muscle activation.

Set Up and Problem Statement. The first rigid body, representing the collarbone, is assumed to be fixed in the inertial frame via a revolute joint modelling the rotation of the torso around the $\boldsymbol{e}_3$-axis, thus the axis of the first revolute joint is $\boldsymbol{n}^1 = \boldsymbol{e}_3$. Collarbone and upper arm are connected via a spherical joint, representing the three-dimensional rotation of the shoulder. A revolute joint serves as the elbow between upper and forearm allowing the forearm to rotate around a prescribed axis $\boldsymbol{n}^2$ fixed in the upper arm.

The actuations via the muscles are modelled as torques acting in the joints. Here, it is assumed that all degrees of freedom, that is the rotations of the collarbone, the shoulder and the elbow, are directly steerable. There is a rotational torque $\boldsymbol{\tau}^{(S)} \in \mathbb{R}^3$ acting in the shoulder joint and two scalar torques $\tau^{(R_1)}, \tau^{(R_2)} \in \mathbb{R}$ acting in the first revolute joint and the elbow joint, respectively. Observe from Figure 7.13 that the system has five generalised joint coordinates $\theta^1, \dots, \theta^5 \in \mathbb{R}$ that constitute the degrees of freedom actuated by the torques. The redundant forces on each body are given by (6.3) where the matrix in (6.4) reduces, due the first body being fixed in space by the revolute joint R_1, to

$$\begin{bmatrix} \boldsymbol{C}^{2,(R_1)}(\boldsymbol{q}) & \boldsymbol{C}^{1,(S)}(\boldsymbol{q}) & \boldsymbol{0} \\ \boldsymbol{0} & \boldsymbol{C}^{2,(S)}(\boldsymbol{q}) & \boldsymbol{C}^{1,(R_2)}(\boldsymbol{q}) \\ \boldsymbol{0} & \boldsymbol{0} & \boldsymbol{C}^{2,(R_2)}(\boldsymbol{q}) \end{bmatrix}. \tag{7.3}$$

The expressions for the nullspace matrix and nodal reparametrisation can be inferred from §5.1, §5.3, and §6.

Jerry: Fonts in the figure are too big.	ToDo

Remark 7.3. For the pitcher, the effect of the actuating torques in the joints on the generalised degrees of freedom takes the form

$$\boldsymbol{P}^T(\boldsymbol{q}) \cdot \boldsymbol{f} = \begin{bmatrix} \tau^{(R_1)} - (\boldsymbol{n}^1)^T \cdot \boldsymbol{\tau}^{(S)} \\ \boldsymbol{\tau}^{(S)} - \tau^{(R_2)} \boldsymbol{n}^2 \\ \tau^{(R_2)} \end{bmatrix}. \tag{7.4}$$

The control torque $\boldsymbol{\tau}^{(S)}$ in the spherical joint acts with different signs on the collarbone and on the upper arm. Only $(\boldsymbol{n}^1)^T \cdot \boldsymbol{\tau}^{(S)}$, the part of $\boldsymbol{\tau}^{(S)}$ in the

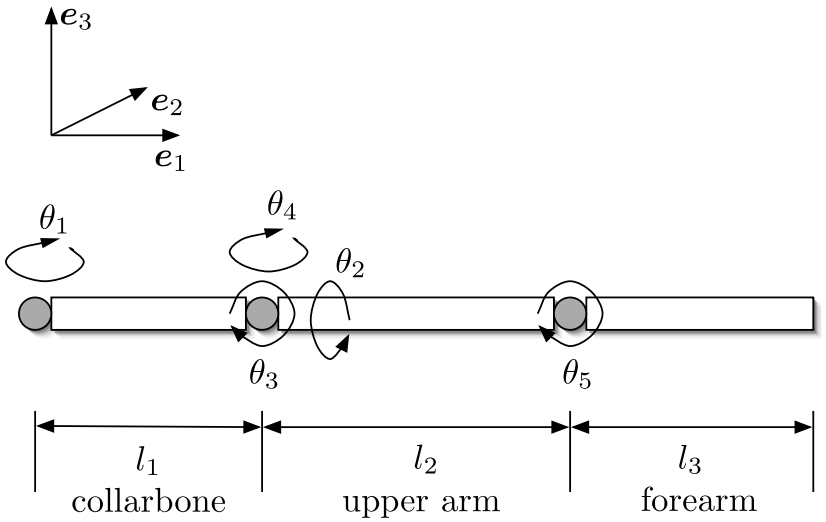

Figure 7.13: The optimal pitch: model for the arm consisting of collarbone, upper arm, and forearm.

direction of $\boldsymbol{n}^1$, influences the collarbone's rotation, since the collarbone is constrained to perform rotational motion around $\boldsymbol{n}^1$ only. Similarly, $\tau^{(R_2)}$ acts on the upper and forearm with different signs, therefore it influences the three generalised degrees of freedom in the shoulder by $\tau^{(R_2)}\boldsymbol{n}^2$.

The pitcher is assumed to begin the motion with prescribed initial configuration and zero velocity. Rather than prescribing final configurations for all present bodies, a limited but not fixed final configuration is defined for the hand position[1], for example positive $\boldsymbol{e}_2$- and $\boldsymbol{e}_3$-position. Due to the human body's anatomy, the relative motion in each joint is limited. To obtain a realistic motion, each generalised configuration variable is bounded, for example the forearm is assumed to bend in only one direction. In addition, the incorporation of bounds on the control torques is needed, since the muscles are not able to create an arbitrary amount of strength.

The goal is to maximise the final momentum of the hand in $\boldsymbol{e}_2$-direction. More specifically, the projected discrete Legendre transform (3.16) is used to compute the discrete objective function $J_d(\boldsymbol{q}_d, \boldsymbol{f}_d) = -\boldsymbol{e}_2^T \cdot \left({}^Q\boldsymbol{p}_N^+\right)_{\text{hand}}$. During the optimisation the final time is free, that means also the optimal duration of the pitch is determined as a variable.

[1]Since the hand is not modelled as a separate rigid body within the system, it is assumed to be located at the endpoint of the forearm.

Problem Solution. The constrained minimisation has been performed with the NAG C library function *nag_opt_nlp_sparse*. Starting from an initial position of the joints as $\theta_0^1 = \theta_0^2 = \theta_0^3 = \theta_0^4 = 0, \theta_0^5 = -\frac{\pi}{4}$, different solutions for the optimal motion are obtained, depending on the initial guess in use. In Figure 7.14 snapshots of a particular locally optimal motion are depicted with the optimal final time $T = 0.415$. The final configuration and momentum of the hand are $\boldsymbol{q}_{hand} = (0.008,\ 0.576,\ 0.453)$ and $\left({}^{Q}\boldsymbol{p}_N^+\right)_{\text{hand}} = (2.323,\ 24.502,\ -5.465)$, respectively. Starting from the initial configuration shown in the first picture, the pitcher strikes his arm out, moves it rearwards, pulls it above his head, before he finally moves his arm like a whip to obtain the necessary swing to maximise the final momentum. The evolution of discrete generalised coordinates and torques can be observed from Figure 7.15. Figure 7.16 illustrates the consistency of angular momentum. Due to the presence of gravitation and the fixing of the chain in space by a revolute joint with rotation axis $\boldsymbol{e}_3$, the only symmetry of the augmented discrete Lagrangian (3.1) is rotation about $\boldsymbol{e}_3$. Therefore, the corresponding component of the angular momentum L_3 changes exactly according to the torque $\tau^{(R_1)}$, applied in the supporting joint. The kinetic energy, which is increasing substantially towards the end of the movement, is shown in Figure 7.17.

Remark 7.4 (Dimension of the constrained optimisation problem)**.** Including the free final time, the number of variables is 361 and the initial conditions and dynamic constraints sum up to 180. In the Lagrange multiplier formulation, one is faced with 3709 variables and 2412 constraints.

To obtain more realistic motions, the next step is to consider more complex models that behave more realistically. For example, instead of modelling the actuation of the limbs by external control torques, the interaction of the muscles and the resulting muscle force can be modelled as well (as investigated in Timmermann [2008]). Due to the constrained formulation of multibody dynamics, model extensions can easily be incorporated by coupling new bodies to the system via constraints.

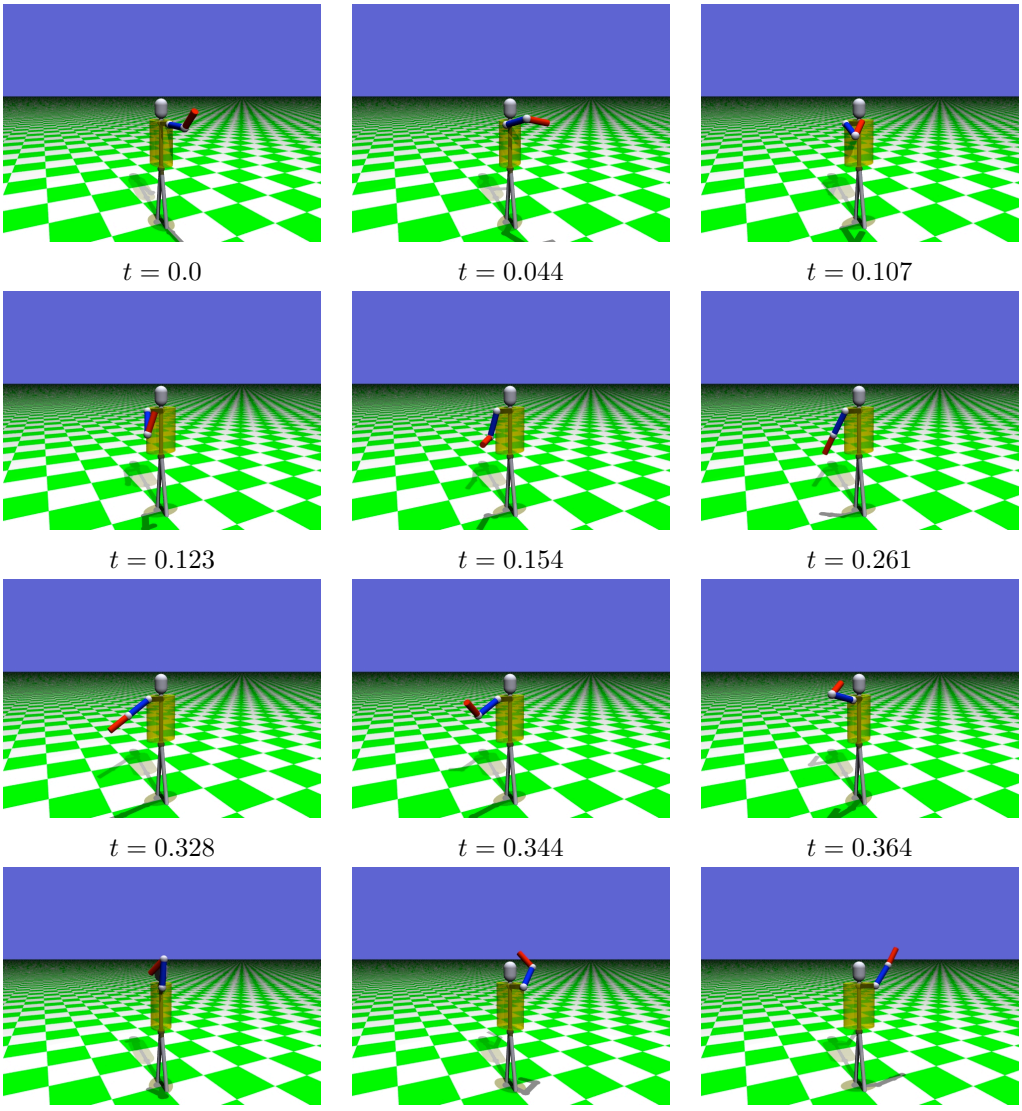

Figure 7.14: The optimal pitch: snapshots of the motion sequence.

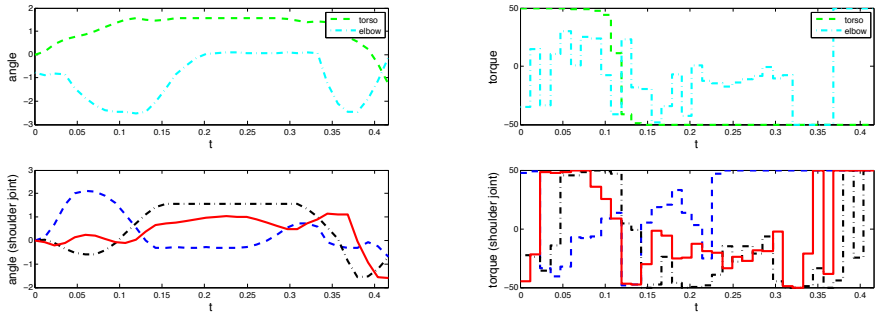

Figure 7.15: The optimal pitch: evolution of discrete generalised coordinates and torques.

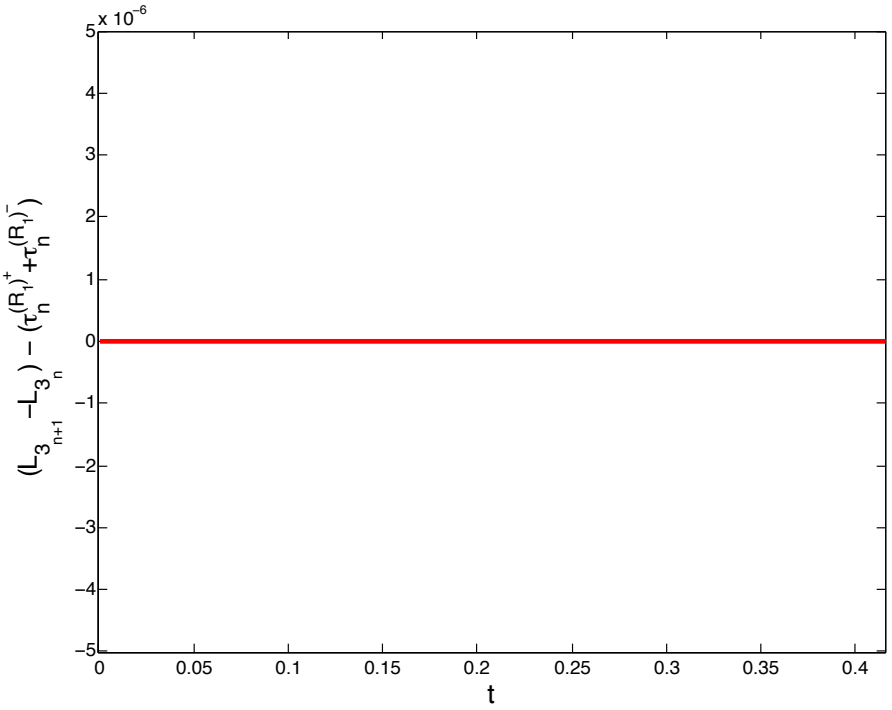

Figure 7.16: The optimal pitch: Consistency of angular momentum.

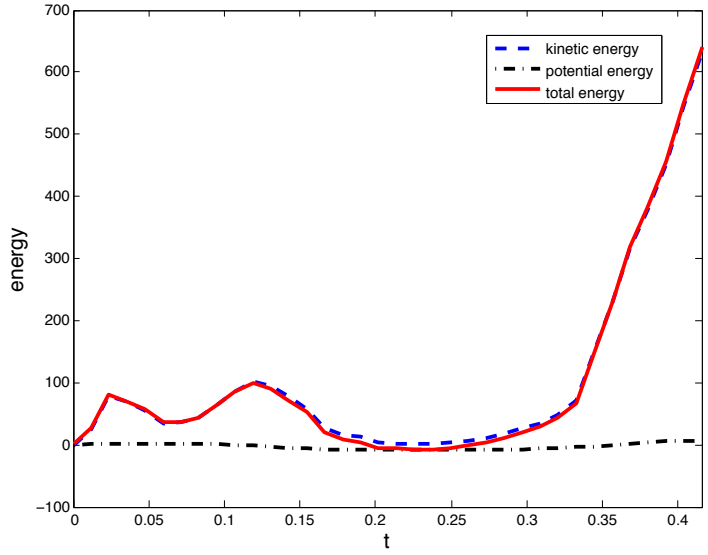

Figure 7.17: The optimal pitch: Evolution of kinetic, potential and total energy computed in terms of the projected conjugate momentum.

8 Conclusion

This paper proposes a new approach to the solution of optimal control problems for constrained mechanical systems via the combination of two recently developed methods: the discrete null space method, which is suitable for the accurate, robust and efficient time integration of such systems, and the optimal control method DMOC.

DMOC is used to compute trajectories for a mechanical system that is optimally guided from an initial to a final configuration via external forces. The given objective function is extremised subject to the reduced discrete dynamic equations of the constrained mechanical system. These are derived from the discrete constrained Lagrange-d'Alembert principle, then the discrete null space method yields reduced time-stepping equations that are used as constraints for the resulting optimisation problem.

The proposed method benefits from an easy derivation and implementation of the constraint equation for the optimisation algorithm and ensures exact constraint fulfilment and structure preserving properties of the computed solutions. In particular, actuating forces being consistent with the specific joint

constraints are given and angular momentum consistency of the resulting time-stepping scheme is proved analytically and verified numerically with a satellite reorientation problem and the optimisation of a pitcher's motion.

References

Antmann, S. [1995], *Nonlinear Problems in Elasticity.* Springer.

Bauchau, O. and L. Trainelli [2003], The vectorial parameterization of rotation, *Nonlin. Dynamics* **1**, 71–92.

Benzi, M., G. Golub, and J. Liesen [2005], Numerical solution of saddle point problems, *Acta Numerica*, 1–137.

Bertsekas, D. [1995], *Nonlinear Programming.* Athena Scientific.

Betsch, P. [2005], The discrete null space method for the energy consistent integration of constrained mechanical systems. Part I: Holonomic constraints, *Comput. Methods Appl. Mech. Engrg.* **194**, 5159–5190.

Betsch, P. and S. Leyendecker [2006], The discrete null space method for the energy consistent integration of constrained mechanical systems. Part II: Multibody dynamics, *Int. J. Numer. Meth. Engng.* **67**, 499–552.

Betsch, P., A. Menzel, and E. Stein [1998], On the parametrization of finite rotations in computational mechanics; A classification of concepts with application to smooth shells, *Comput. Methods Appl. Mech. Engrg.* **155**, 273–305.

Betsch, P. and P. Steinmann [2001], Constrained integration of rigid body dynamics, *Comput. Methods Appl. Mech. Engrg.* **191**, 467–488.

Betsch, P. and P. Steinmann [2002], Conserving properties of a time FE method – Part III: Mechanical systems with holonomic constraints, *Int. J. Numer. Meth. Engng.* **53**, 2271–2304.

Betts, J. [1998], Survey of numerical methods for trajectory optimization, *Journal of Guidance, Control, and Dynamics* **21**.

Biegler, L. [1984], Solution of dynamic optimization problems by successive quadratic programming and orthogonal collocation, *Comput. Chem. Engng.* **8**, 243–248.

Binder, T., L. Blank, H. Bock, R. Bulirsch, W. Dahmen, M. Diehl, T. Kronseder, W. Marquardt, J. Schlöder, and O. vonStryk [2001], Introduction to model based optimization of chemical processes on moving horizons, *Online Optimization of Large Scale Systems: State of the Art*, 295–340. http://www.zib.de/dfg-echtzeit/Publikatio nen/Preprints/Preprint-01-15.html.

Bock, H. and K. Plitt [1984], A multiple shooting algorithm for direct solution of optimal control problems. In *Proc. 9th IFAC World Congress Budapest*, pages 243–247.

Bou-Rabee, N. and H. Owhadi [2007], Stochastic variational partitioned Runge-Kutta integrators for constrained systems. submitted for publication.

Bou-Rabee, N. and H. Owhadi [2008], Stochastic variational integrators, *IMA Journal of Numerical Analysis*.

Bullo, F. and A. Lewis [2004], *Geometric Control of Mechanical Systems*. Springer.

Deuflhard, P. [1974], A modified Newton method for the solution of ill-conditioned systems of nonlinear equations with application to multiple shooting, *Numer. Math.* **22**, 289–315.

Gill, P., L. Jay, M. Leonard, L. Petzold, and V. Sharma [2000], An SQP method for the optimal control of large-scale dynamical systems, *J. Comp. Appl. Math.* **20**, 197–213.

Gill, P., W. Murray, and M. Saunders [1997], SNOPT: An SQP algorithm for large-scale constrained optimization, *Numerical Analysis Report, Department of Mathematics, University of California, San Diego, La Jolla, CA* **97-2**.

Goldstein, H., C. Poole, and J. Safko [2002], *Classical Mechanics*. Addison Wesley.

Gonzalez, O. [1999], Mechanical systems subject to holonomic constraints: differential-algebraic formulations and conservative integration, *Physica D* **132**, 165–174.

Hairer, E., C. Lubich, and M. Roche [1989], *The numerical solution of differential algebraic equations by Runge-Kutta methods*. Springer.

Hicks, G. and W. Ray [1971], Approximation methods for optimal control systems, *Can. J. Chem. Engng.* **49**, 522–528.

Junge, O., J. Marsden, and S. Ober-Blöbaum [2005], Discrete mechanics and optimal control. In *Proceedings of the 16th IFAC World Congress*, Prague.

Junge, O. and S. Ober-Blöbaum [2005], Optimal Reconfiguration of Formation Flying Satellites. In *IEEE Conference on Decision and Control and European Control Conference ECC*, Seville, Spain.

Junge, O. and S. Ober-Blöbaum [2006], Optimal reconfiguration of formation flying spacecraft - a decentralized approach. In *Proceedings of the IEEE Conference on Decision and Control and European Control Conference ECC*, San Diego, USA.

Kanso, E. and J. Marsden [2005], Optimal motion of an articulated body in a perfect fluid. In *IEEE Conference on Decision and Control and European Control Conference ECC 2005*, Seville, Spain.

Kraft, D. [1985], On converting optimal control problems into nonlinear programming problems, *Computational Mathematical Programming* **F15**, 261–280.

Leimkuhler, B. and S. Reich [2004], *Simulating Hamiltonian Dynamics*. Cambridge University Press.

Leineweber, D., I. Bauer, H. Bock, and J. Schlöder [2003], An efficient multiple shooting based reduced SQP strategy for large-scale dynamic process optimization. Part I: Theoretical aspects, *Comp. Chem. Eng.* **27**, 157–166.

Leyendecker, S. [2006], *Mechanical integrators for constrained dynamical systems in flexible multibody dynamics*, PhD thesis, University of Kaiserslautern.

Leyendecker, S., P. Betsch, and P. Steinmann [2004], Energy-conserving integration of constrained Hamiltonian systems – a comparison of approaches, *Comput. Mech.* **33**, 174–185.

Leyendecker, S., P. Betsch, and P. Steinmann [2006], Objective energy-momentum conserving integration for the constrained dynamics of geometrically exact beams, *Comput. Methods Appl. Mech. Engrg.* **195**, 2313–2333.

Leyendecker, S., P. Betsch, and P. Steinmann [2008], The discrete null space method for the energy consistent integration of constrained mechanical systems. Part III: Flexible multibody dynamics, *Multibody System Dynamics* **19**, 45–72.

Leyendecker, S., J. Marsden, and M. Ortiz [2008], Variational integrators for constrained dynamical systems, *ZAMM.* accepted for publication.

Leyendecker, S., S. Ober-Blöbaum, J. Marsden, and M. Ortiz [2007], Discrete mechanics and optimal control for constrained multibody dynamics. In *Proceedings of the 6th International Conference on Multibody Systems, Nonlinear Dynamics, and Control, ASME International Design Engineering Technical Conferences*, Las Vegas, Nevada.

Luenberger, D. [1984], *Linear and Nonlinear Programming*. Addison-Wesley.

Marsden, J. E. and T. S. Ratiu [1999], *Introduction to Mechanics and Symmetry*, volume 17 of *Texts in Applied Mathematics; 1994, Second Edition, 1999*. Springer-Verlag.

Marsden, J. and M. West [2001], Discrete mechanics and variational integrators, *Acta Numerica* **10**, 357–514.

Ober-Blöbaum, S. [2008], *Discrete mechanics and optimal control*, PhD thesis, University of Paderborn.

Petzold, L. and P. Lostedt [1986], Numerical solution of nonlinear differential equations with algebraic constraints II: Practical implications, *SIAM J. Sci. Comput.* **7**, 720–733.

Reich, S. [1996], Symplectic integrators for systems of rigid bodies, *Fields Institute Commun.* **10**, 181–191.

Rheinboldt, W. [1997], Solving Algebraically Explicit DAEs with the MANPAK-Manifold-Algorithms, *Computers Math. Applic.* **33**, 31–43.

Schittkowski, K. [1980], *Nonlinear programming codes, Lecture Notes in Economics and Mathematical Systems*, volume 183, viii+242. Springer.

Stoer, J. and R. Bulirsch [2002], *Introduction to numerical analysis*, volume 12, xvi+744. Springer.

Timmermann, J. [2008]. Die nullraum-methode in kombination mit dmoc zur optimalen steuerung mechanischer systeme mit holonomen zwangsbedingungen, 2008. Diplomarbeit, Universität Paderborn.

von Stryk, O. [1991], Numerical solution of optimal control problems by direct collocation, *Optimal control (Freiburg, 1991), Internat. Ser. Numer. Math.*, 129–143.

Wendlandt, J. and J. Marsden [1997], Mechanical Integrators Derived from a Discrete Variational Principle, *Physica D* **106**, 223–246.

`Jerry: Any of these next references relevant?`	ToDo

Krysl, P. [2005], Explicit momentum-conserving integrator for dynamics of rigid bodies approximating the midpoint Lie algorithm, *Internat. J. Numer. Methods Engrg.* **63**, 2171–2193.

Krysl, P. [2006], Direct time integration of rigid body motion with discrete-impulse midpoint approximation: explicit Newmark algorithms, *Comm. Numer. Methods Engrg.* **22**, 441–451.

Krysl, P. [2008], Dynamically equivalent implicit algorithms for the integration of rigid body rotations, *Comm. Numer. Methods Engrg.* **24**, 141–156.

Bou-Rabee, N. M. and J. Marsden [2008], Reduced Hamilton-Pontryagin variational integrators, *Found. Comput. Math. (to appear)*.